HYDROLOGICAL PROCESSES
Hydrol. Process. (2012)
Published online in Wiley Online Library
(wileyonlinelibrary.com) DOI: 10.1002/hyp.9661

Impacts of climate change in three hydrologic regimes in British Columbia, Canada

Markus Schnorbus,[1]* Arelia Werner[1] and Katrina Bennett[2]

[1] *Pacific Climate Impacts Consortium, University House 1, University of Victoria, PO Box 3060 Stn CSC, Victoria, BC V8W 3R4, Canada*
[2] *International Arctic Research Center, University of Alaska Fairbanks, 930 Koyukuk Drive, PO Box 757340, Fairbanks, AK 99775–7340, USA*

Abstract:

Hydrologic modelling has been applied to assess the impacts of projected climate change within three study areas in the Peace, Campbell and Columbia River watersheds of British Columbia, Canada. These study areas include interior nival (two sites) and coastal hybrid nival–pluvial (one site) hydro-climatic regimes. Projections were based on a suite of eight global climate models driven by three emission scenarios to project potential climate responses for the 2050s period (2041–2070). Climate projections were statistically downscaled and used to drive a macro-scale hydrology model at high spatial resolution. This methodology covers a large range of potential future climates for British Columbia and explicitly addresses both emissions and global climate model uncertainty in the final hydrologic projections. Snow water equivalent is projected to decline throughout the Peace and Campbell and at low elevations within the Columbia. At high elevations within the Columbia, snow water equivalent is projected to increase with increased winter precipitation. Streamflow projections indicate timing shifts in all three watersheds, predominantly because of changes in the dynamics of snow accumulation and melt. The coastal hybrid site shows the largest sensitivity, shifting to more rainfall-dominated system by mid-century. The two interior sites are projected to retain the characteristics of a nival regime by mid-century, although streamflow-timing shifts result from increased mid-winter rainfall and snowmelt, and earlier freshet onset. Copyright © 2012 John Wiley & Sons, Ltd.

KEY WORDS climate change; hydrologic modelling; hydrology; streamflow; snow; British Columbia

Received 2 March 2012; Accepted 20 November 2012

INTRODUCTION AND BACKGROUND

Historical changes to climate and hydrology have already been documented in British Columbia (BC) and western North America (e.g. Barnett *et al*., 2008). Although they are affected by natural climate variability, such as El Niño/Southern Oscillation (ENSO) and the Pacific Decadal Oscillation (PDO) (Moore and McKendry 1996; Fleming *et al*., 2007), recent hydro-climatic trends in western North America have been attributed to climate change, predominantly in the form of increased regional warming (Barnett *et al*., 2008; Bonfils *et al*., 2008; Pierce *et al*., 2008). According to the Intergovernmental Panel on Climate Change (IPCC) Fourth Assessment Report, it is now 'very likely' that this observed widespread warming of the atmosphere and oceans is due to anthropogenic greenhouse gas emissions, predominantly from fossil fuel use (IPCC 2007).

Throughout most of BC, seasonal runoff is either snow dominated (nival regimes) or snow influenced (hybrid nival–pluvial or nival–glacial regimes) (Eaton and Moore, 2010). Within such regimes, documented hydrologic trends over recent decades generally include decreasing snowpack, earlier onset of spring melt, decreasing summer flow and delayed onset of autumn flows, resulting in an extension of the dry hydrologic season (Whitfield and Cannon 2000; Barnett *et al*., 2005; Regonda *et al*., 2005; Déry *et al*., 2009). Climate change trends will persist with continued emissions of greenhouse gases, and further changes in regional temperature and precipitation patterns are expected to affect the regional hydrologic cycle, with possible impacts to various water-related resources and water-dependent activities (Cohen *et al*., 2000; Mote *et al*., 2003; Hayhoe *et al*., 2004; Payne *et al*., 2004; Merritt *et al*., 2006; Schindler and Donahue 2006; Toth *et al*., 2006; Milly *et al*., 2008; Hamlet *et al*., 2010; Mantua *et al*., 2010; Vano *et al*., 2010a, b).

The hydro-climatology of BC is complex because of its close proximity to the Pacific Ocean, mountainous terrain and large latitudinal expanse. The hydrologic response to climatic change in BC is therefore expected to be influenced by regional variability in future temperature and precipitation changes and by regional variation in physical geography. For instance, projected changes in snow storage dynamics are strongly affected by elevation-based temperature gradients, generating large spatial variation in regions of complex topography (Kim, 2001; Knowles and Cayan, 2004; Mote *et al*., 2005; Chang and Jung, 2010). Also, relatively warm coastal rainfall-dominated (i.e. pluvial) and hybrid nival–pluvial systems may tend to be more sensitive to regional temperature, precipitation and rainfall trends (Whitfield *et al*., 2002).

Although many water-related issues are germane to BC, sustainable and self-sufficient generation of electricity has been identified as a significant concern and a major policy objective for the BC government. Hydroelectricity is BC's largest source of electric power generation, and assets in the Peace River (PR) and Upper Columbia River (UCR)

*Correspondence to: Markus Schnorbus, Pacific Climate Impacts Consortium, University of Victoria, PO Box 3060 Stn CSC, Victoria, BC, V8W 3R4, Canada.
E-mail: mschnorb@uvic.ca

watersheds account for 85% of this generation. However, a number of generation sites are also located within smaller drainages distributed throughout the southern coastal region of the province, such as the Campbell River (CR) watershed. Consequently, an understanding the hydrologic implications of climate change in these diverse watersheds is critical for effectively and sustainably managing the province's hydro-generation resources.

This paper describes the application of a high-resolution, physically based macro-scale hydrologic model to assess the hydrologic impacts of climate change within the PR, UCR and CR systems, three distinct physiographic regions. The hydrologic modelling is driven by climate projections statistically downscaled from a suite of eight global climate models (GCMs) driven by multiple emission scenarios. Streamflow projections were made for several project sites within the study areas, corresponding to current generation sites, potential sites for future hydroelectricity development and several natural drainages. Our choice of methodology and the use of recent climate projections expands upon past climate change impact studies conducted for these specific study areas (e.g. Hamlet and Lettenmaier, 1999; Loukas *et al*., 2002a, b; Payne *et al*., 2004; Pietroniro *et al*., 2006; Toth *et al*., 2006). Further, this study also represents the first time that potential climate change impacts have been addressed and compared in all three regions simultaneously using consistent methodology.

STUDY AREAS

Hydrologic impacts were modelled in three study areas located within the PR, CR and UCR basins in BC (Figure 1). These three study areas represent a range of

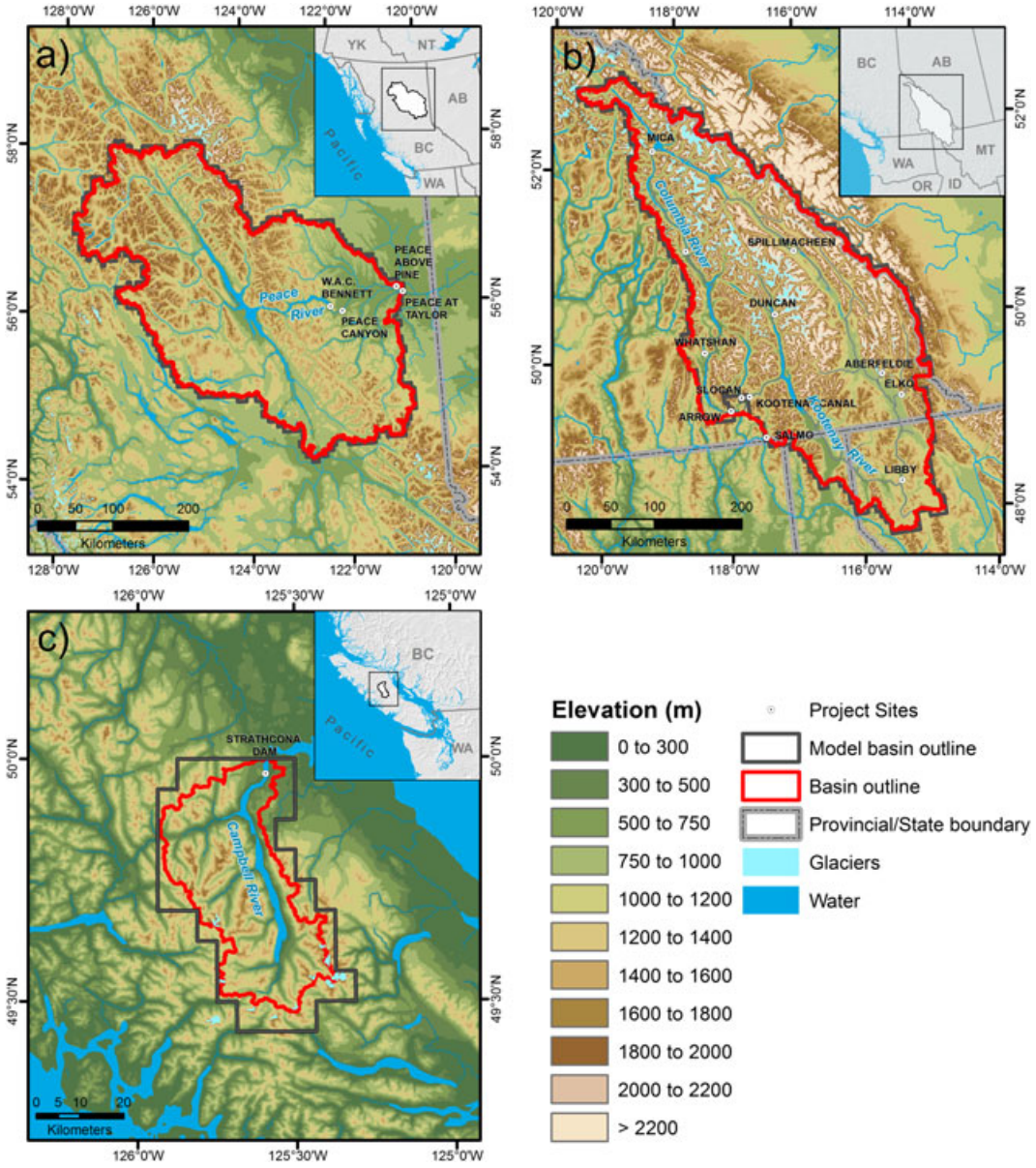

Figure 1. Study area maps, showing the three study area watersheds and project sites of the (a) Peace River, (b) Upper Columbia River and (c) Campbell River. The three example project sites referred to specifically herein are the Peace River at the W.A.C Bennett Dam (W.A.C. BENNETT in panel (a)), the Columbia River at Mica Dam (MICA in panel (b)) and the Campbell River at Strathcona Dam (STRATHCONA DAM in panel (c))

climatic, topographic and physiographic conditions. Basin physiography and annual hydro-climatology are summarized in Table I, and monthly hydro-climatology is shown in Figure 2.

The PR study area is located in interior north-eastern BC and encompasses the drainage area upstream of Taylor, BC (Figure 1). The region has a continental climate (Demarchi 1996), with monthly average temperatures ranging from −12.0 °C in January to 12.3 °C in July. Precipitation follows a seasonal pattern of summer maximum and spring minimum (Figure 2). The PR has the lowest average temperature and precipitation of all three study areas. It has a nival regime, with approximately 54% of the annual precipitation (440 mm) falling as snow (mostly during October–April) and 64% of the natural streamflow occurring during the freshet months of May–July (Figure 2). Low flows occur during the winter and early spring.

The UCR study area is located in south-eastern BC and occupies the drainage area upstream of the confluence of the Kootenay and Columbia Rivers (Figure 1). The UCR has the highest elevations of the three study areas (Table I) and has a continental climate (Demarchi 1996). Monthly average temperature ranges from −9.4 °C in January to 13.4 °C in July (Figure 2). Precipitation experiences seasonal variation and is highest in the winter. Approximately 65% of the annual precipitation falls as snow, with snowfall possible throughout the year. In addition, approximately 4% of the area is covered by glaciers. Consequently, natural streamflow at many locations in the UCR exhibits a glacial–nival regime, where the hydrologic cycle is dominated by the spring freshet, with a gradual recession in flow during the late summer and fall and lowest flow occurring during the winter (Figure 2).

The CR is a relatively small watershed that drains the mountains of central Vancouver Island (Figure 1). The region exhibits a typical coastal climate, with mild, wet winters and warm dry summers (Figure 2) (Demarchi 1996). The CR has the warmest temperatures and receives the most precipitation of all three study areas. Monthly average temperatures range from −1.8 °C in December to 14.9 °C in August. Precipitation has a pronounced seasonal distribution, with 78% of the precipitation falling during the 6-month period of October–March. Snowfall accounts for 23% (680 mm) of the annual precipitation, such that natural streamflow exhibits a hybrid nival–pluvial regime, peaking in both the fall and spring (Figure 2). Approximately 32% of the annual discharge occurs during the freshet months of May, June and July, with June receiving the highest discharge during the year. Rainfall runoff during the fall months of October–November accounts for 31% of the annual discharge. The CR is at the lowest elevation of the three study areas.

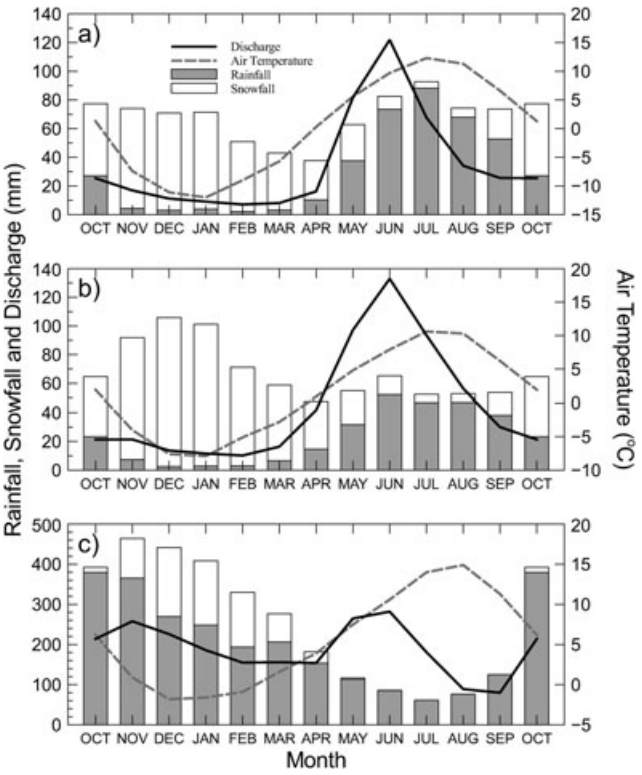

Figure 2. Area-average 1961–1990 monthly climatology for rainfall, snowfall, temperature and discharge for the (a) Peace River, (b) Upper Columbia River and (c) Campbell River study areas. Rainfall and snowfall are presented as stacked bars (i.e. rainfall + snowfall = precipitation). Total discharge for each study area estimated from available naturalized discharge at (a) Peace River at Taylor (PEACE AT TAYLOR in Figure 1; 1968–1990), (b) Columbia River at outlet of Arrow Lakes plus Kootenay River at Kootenay Canal plus Slocan River (ARROW, KOOTENAY CANAL and SLOCAN, respectively, in Figure 1; 1984–1990) and (c) Campbell River at Strathcona Dam (STRATHCONA DAM in Figure 1; 1963–1990)

Table I. Study area physical description and 1961–1990 annual hydro-climatology

	Study area		
Variable	PR	UCR	CR
Drainage area (km^2)	101 000	104 000	1190
Minimum elevation (m)	400	420	140
Median elevation (m)	1200	1600	1000
Maximum elevation (m)	2800	3550	2200
Annual average temperature (°C)	0.2	1.9	5.6
Annual precipitation (mm)	810	930	2960
Annual snowfall (mm)	440	610	680
Annual discharge (m^3/s)	1360	2020	75
Hydrologic regime	Nival	Nival–glacial	Nival–pluvial

Streamflow projections are provided for three example locations corresponding to current hydroelectric power generation sites, one within each study area. These sites are the PR at W.A.C. Bennett Dam (referred to as BD), the UCR at Mica Dam (MD) and the CR at Strathcona Dam (referred to as SD) (Figure 1). BD has a nival regime that encompasses a drainage area of 72078 km^2 (71% of the PR study area). MD has a drainage area of 21134 km^2 (20% of the UCR study area) and, with 8% of its area covered by glaciers, exhibits a glacial–nival regime. The SD drains the entire 1190 km^2 of the CR study area.

METHODS

Climate projections

Our study uses GCM output contributed by the World Climate Research Programme through its Coupled Model Intercomparison Project phase 3 multi-model dataset (Meehl *et al*., 2007). The current study employed output from a subset of eight participating models. The process of GCM selection, which is based on model performance over western North America, is described in detail by Werner (2011). Future emissions and radiative forcing trajectories are based on the A1B, A2 and B1 scenarios described in the IPCC Special Report on Emissions Scenarios (SRES) (Nakićenović and Swart, 2000). These scenarios reflect a range of low, medium and high potential future forcings (B1, A1B and A2, respectively) by the end of the 21st century. However, the A1B and A2 scenarios have similar emissions until mid-century, only diverging substantially after 2050. With one exception, we employ a single run from each GCM for each of the three emission scenarios, for a total of 23 climate projections, which are summarized in Table II. The selection of GCMs and emission scenarios covers a large range in potential projected future climates for BC. Climate projections were obtained from the GCMs as monthly time series of temperature and precipitation for 1950–2098. Climate projections, and subsequent hydrologic projections, from the final ensemble of GCM runs are treated as statistically indistinguishable (Annan and Hargreaves, 2010; Knutti *et al*., 2010).

The monthly GCM climate projections of temperature and precipitation were spatially downscaled using the statistical Bias-corrected Spatial Disaggregation (BCSD) approach (Wood *et al*., 2002, 2004; Salathé, 2005). This technique is computationally efficient and was utilized to generate a daily time series of gridded temperature and precipitation for the period 1950–2098 for each GCM scenario run at the resolution of the hydrologic model (1/16°) (see Section on Hydrology Model and Werner 2011). Climate projections are bias corrected by quantile mapping monthly GCM precipitation and temperature to gridded observed data, with the same mapping applied to future projections. This correction explicitly allows for the mean and variability of a GCM to evolve while matching all moments between GCM and observations during the calibration period. Note that the bias correction step corrects GCM output to observed data but does not account for potential bias in the observed data itself, which can be large, particularly for precipitation in regions of complex topography (e.g. Adam *et al*., 2006; Stahl *et al*., 2006; see Section on Model Calibration and Performance). BCSD reproduces the large-scale GCM trends interpolated to the downscaling target resolution (Maurer and Hidalgo, 2008; Werner, 2011) but does not address potential local detail or variability in the climate response, such as possible variations in temperature or precipitation trends with elevation (e.g. Bürger *et al*., 2011). Temporal disaggregation is performed via random sampling of historical months, where each day in the selected month is rescaled (multiplicative for precipitation and additive for temperature) to match the projected monthly total precipitation and average temperature. Thus, BCSD downscaling does not reflect potential future changes to the statistical properties of daily weather projected by individual GCMs (Maurer and Hidalgo, 2008), but it does capture the transient nature of the emission scenarios and the simulated altered monthly statistics. Although BCSD can use daily GCM data directly, daily GCM output is less widely available and arguably less skillful in simulating daily precipitation, and the assumption of climatological daily variability has proven reasonable in past hydrologic applications (Leavesley, 1994; Wood *et al*., 2002; Maurer and Hidalgo, 2008).

The downscaled regional climate projections were used to force a hydrologic model, producing an ensemble of 23 hydrologic projections for each study area (composed of three scenario-based ensembles of 8, 8 and 7 projections for A1B, A2 and B1, respectively). Changes in the

Table II. Global climate model and SRES scenario selection summary

Model ID	Modelling centre, country and model	SRES scenarios	Primary reference
CGCM3	Canadian Centre for Climate Modelling and Analysis (Canada), CGCM3.1 (T47)	A2, A1B, B1	Scinocca *et al.* (2008)
CCSM3	National Center for Atmospheric Research (USA), CCSM3	A2, A1B, B1	Collins *et al.* (2006)
CSIRO	CSIRO Atmospheric Research (Australia), CSIRO Mk3.0	A2, A1B, B1	Rotstayn *et al.* (2010)
ECHAM5	Max Planck Institute for Meteorology (Germany), ECHAM5/MPI-OM	A2, A1B, B1	Roeckner *et al.* (2006)
GFDL	NOAA Geophysical Fluid Dynamics Laboratory (USA), GFDL-CM2.1	A2, A1B, B1	Delworth *et al.* (2006)
HADCM3	Hadley Centre for Climate Prediction and Research (UK), HadCM3	A2, A1B, B1	Collins *et al.* (2001)
HADGEM	Hadley Centre for Climate Prediction and Research (UK), HadGEM1	A2, A1B	Martin *et al.* (2006)
MIROC	Center for Climate Systems Research (Japan), MIROC3.2 (medres)	A2, A1B, B1	K-1 Model Developers (2004)

various components of the hydrologic cycle were quantified by comparing temperature, precipitation, snow, runoff and streamflow from two 30-year periods within the simulations that represent historical and future conditions. The focus is on mid-21st century changes, where the future period of 2041–2070 (the 2050s) is compared with the historical baseline of 1961–1990 (the 1970s).

Uncertainty is an inherent component of the process of obtaining hydrologic projections. The methodology of using an ensemble of multiple GCMs coupled to three emission scenarios explicitly addresses both emissions and GCM structural uncertainty. However, reliance on only one downscaling technique and one hydrologic model means that our results do not incorporate uncertainties from these two sources. Nevertheless, recent research suggests that differences in global climate response to greenhouse forcings between different GCMs are the largest source of uncertainty, and uncertainties attributed to downscaling, emission scenarios and hydrologic modelling are of lesser magnitude (Wilby, 2005; Prudhomme and Davies, 2009; Blöschl and Montanari, 2010; Bennett *et al*., 2012). Additional unquantified uncertainty likely arises from assumptions of stationarity that are implicit in the downscaling and hydrologic modelling parameterizations.

Historical climate data

Although hydrologic projections are simulated by forcing the hydrologic model with downscaled GCM projections, calibration of both the hydrologic model and BCSD requires historical climate data. This climate data are in the form of daily gridded surfaces of minimum and maximum temperatures, daily precipitation accumulation and daily average wind speed at the spatial resolution of 1/16°. The daily surfaces were produced following the technique of Maurer *et al*. (2002) and Hamlet and Lettenmaier (2005) (see Schnorbus *et al*. (2011) for details). The technique involves spatial interpolation of daily temperature and precipitation station data (sources from Environment Canada, US Co-operative station network and BC Hydro), temporal homogenization of the raw fields to remove interpolation artefacts introduced by using a temporally varying mix of stations and corrections for topographic effects using ClimateWNA, a 1961–1990 PRISM-based high-resolution climatology for western Canada (Daly *et al*., 1994; Wang *et al*., 2006).

Hydrology model

The Variable Infiltration Capacity (VIC) hydrologic model (Liang *et al*., 1994, 1996) is used to quantify the hydrologic impacts of climate change. The VIC model is a spatially distributed macro-scale hydrologic model that was originally developed as a soil–vegetation–atmosphere transfer scheme for GCMs. The VIC model has been previously applied to evaluate climate change impacts on river systems globally (Nijssen *et al*., 2001) and in the mountainous western United States and southern BC (Hamlet and Lettenmaier, 1999; Christensen *et al*., 2004; VanRheenen *et al*., 2004; Hamlet *et al*., 2005; Elsner *et al*., 2010). The VIC model is applied at a resolution of 1/16° (approximately 27–31 km^2, depending upon latitude) and run at a daily timestep (1-h timestep for the snow model).

Model set-up. Soil classification and parametrization were based primarily on physical soil data from the Soils Program in the Global Soil Data Products CD-ROM (Global Soil Data Task Group 2000). The soil data contained in the Soils Program are from a global pedon database produced by the International Soil Reference and Information Centre (Batjes, 1995) and the FAO-UNESCO Digital Soil Map of the World (FAO 1995). Physical soil parameters, such as hydraulic conductivity, bulk density, porosity, wilting point and soil textures, were extracted from the Soils Program, interpolated from 5×5 arc-min (1/12°) to the 1/16° VIC grid, and then used to generate the values required to run the VIC model.

Land cover within the VIC model is described by assigning one or more vegetation classes to each model grid cell. Land cover information from the Earth Observation for Sustainable Development of Forests project was used as the basis for the VIC land cover classification (Wulder *et al*., 2003). Monthly leaf area index (LAI) values were calculated from a Canada-wide, 1-km resolution time series of 10-day LAI produced by Natural Resources Canada, which are based on SPOT-4 VEGETATION satellite-based data collected from 1998–2004 (Fernandes *et al*., 2003). The VIC model estimates the fraction of shortwave radiation transmitted through the overstory as a function of LAI by using the Beer–Lambert model (Liang *et al*., 1994), with parameter values taken from Schnorbus *et al*. (2010). Roughness and displacement height were set as functions of vegetation height (Campbell and Norman, 1998). Vegetation architectural and resistance parameters were taken from Dickinson *et al*. (1991), Ducoudré *et al*. (1993) and Shuttleworth (1993). Land cover albedo values were obtained from Bras (1990), Campbell and Norman (1998) and Roberts (2000). Rooting depths and root distributions were also specified for each vegetation class, such that short vegetation draws moisture mainly from the upper soil layer, whereas trees draw moisture from deeper soil layers (Jackson *et al*., 1996). Although it is recognized that climatic change may influence future forest dynamics (e.g. Carroll *et al*. 2006; Huang *et al*., 2007; Marlon *et al*., 2009; Gonzalez *et al*., 2010), incorporating dynamic forest cover is not within the scope of the current study, and forest cover parametrization is fixed at *ca* 2000 conditions throughout the projection timeframe (1950–2098).

Topographic parameters were derived from a post-processed version (version 3) of the Shuttle Radar Topography Mission-based 90-m digital elevation model (Farr *et al*., 2007) obtained from the Consultative Group on International Agricultural Research – Consortium for

Spatial Information (http://srtm.csi.cgiar.org/). An average elevation was calculated for each grid cell. In areas of high relief, variation in sub-grid topography is simulated via the application of elevation bands, with the number of bands ranging from one in cells with low relief to five in cells with high relief. The number of bands per cell was constrained such that the difference in mean elevation between adjacent bands was $\geq$500 m. During model run time, input values of temperature and precipitation for each grid cell are interpolated to each elevation band. Precipitation is adjusted for elevation by using a precipitation gradient estimated from the ClimateWNA annual 1961–1990 precipitation climatology. Grid cell input temperature is lapsed to each individual band at a rate of 6.5 °C/km, applied over the difference between the mean band and the mean grid cell elevations.

The surface-routing network between grid cells is conceptually defined by specifying a flow direction and distance for each 1/16° cell. Surface routing is carried out using the linearized Saint-Venant equations. The Saint-Venant equations are parametrized by specifying values of wave velocity and flow diffusion for each grid cell. Routing parameters were assigned by classifying routing segments as either river channels or natural lakes (e.g. Duncan Lake, Kootenay Lake and Arrow Lakes), with separate parameter sets for each; values were adopted from Schnorbus *et al.* (2010). Note that routing does not include the effects of regulation, extraction or diversion and, thus, represents only 'natural' flow conditions. A full description of the routing model methodology can be found in Lohmann *et al.* (1996).

Glaciers. A simple, conceptual representation of glacier mass balance has been introduced into VIC for projecting the hydrologic response in the UCR system to climate change. Glaciers are modelled by using perennial snow in conjunction with VIC's built-in snow-modelling routines. A portion of the VIC model grid cells in the UCR study area was identified as glacier cells and used to form a glacier mask. The glacier mask includes grid cells with more than 33% area composed of glaciated terrain, on the basis of the 1 : 250 000 Baseline Thematic Mapping version 1 land cover dataset (BC Integrated Land Management Bureau 1995). The 33% threshold was chosen such that the actual glacier surface area and the area of the VIC glacier mask for the Upper Columbia domain would be roughly equivalent (approximately 3700 km^2). This provided a *ca* 1995 glacier mask composed of 135 grid cells (out of a total of 3561 cells). The additional water equivalent required to add glaciers to these grid cells was estimated from volume area scaling (Bahr *et al.*, 1997; Stahl *et al.*, 2008) based on the glacier surface areas in the Baseline Thematic Mapping dataset. The estimated glacier volume was converted to an equivalent depth assuming an average glacier ice density of 700 kg/m^3 (Schiefer *et al.*, 2007). In this scheme, regional changes in glacier area and volume are calculated via mass balance changes in individual grid cells (more specifically, in individual elevation bands within grid cells), and glacier dynamics (i.e. the transport of ice mass from the accumulation zone to the ablation area within and between grid cells) is neglected (termed 'non-dynamic downwasting' by Huss *et al.*, 2010).

The lack of historical glacier inventory data introduces a considerable challenge when specifying an initial glacier state in transient hydrologic projections. Therefore, hydrologic projections were conducted in two phases, both initialized with the 1995 glacier state. Hydrologic projections during the historical period were initialized in 1950 and run from 1 October 1950 to 30 September 1995. Future projections were re-initialized in 1995 and run from 1 October 1995 to 31 December 2098. It is recognized that this process does not explicitly capture the historical trajectory of glacier area and volume within the UCR (Dyurgerov and Meier 2005; Kaser *et al.*, 2006; Schiefer *et al.*, 2007). However, the work of Debeer and Sharp (2007), which investigated changes in glacier area between the years 1951/1952 and 2001 in south-eastern BC, indicates a trend in glacier area of approximately −6% in the UCR region, such that the use of a 1995 glacier mask underestimates 1950 glacier area in the UCR only by roughly 220 km^2 (approximately eight grid cells, assuming 28 km^2/cell). However, this trend may be underestimated as Debeer and Sharp (2007) did not examine area changes in the larger glaciers in the northern part of the UCR.

In this simplified scheme, seasonal snow and glacier water equivalent in the UCR are modelled as combined snow water equivalent (SWE). Hence, to assess changes in seasonal snow and glacier mass separately, bulk-simulated SWE must be partitioned into seasonal and perennial components. This is achieved by taking annual minimum SWE in any given year as a proxy for the glacier state, where the annual minimum is assumed to occur at the beginning of the water year on 1 October. Therefore, changes in glacier mass can be inferred using changes in annual minimum SWE. Conversely, seasonal SWE at any given time in any given water year is estimated as the difference between bulk and annual minimum SWE values. Hereafter, any results or discussion regarding snow in the UCR assumes seasonal snow, unless specifically stated otherwise.

Model calibration and performance. Initial calibration involved manual adjustment of global parameters controlling regional snow accumulation and melt; those being snow albedo decay and precipitation phase temperature thresholds. The albedo decay values of Schnorbus *et al.* (2010) for the Fraser River basin were found suitable and adopted for the PR, UCR and CR study areas. Syntheses of surface weather observations in Canada (Bartlett *et al.*, 2006) and the United States (Auer, 1974) suggest that the temperature range for mixed rain/snow generally occurs between 0 and 6 °C on an annual basis, and those values appear appropriate for the interior basins of the PR and UCR. However, temperature thresholds are known to vary regionally (Barry, 1992; Kienzle, 2008), and the temperature thresholds in the

coastal CR were found to be −0.5–4 °C. An assessment of VIC's snow simulation performance in the PR and UCR study areas is provided in Figure 3. Comparison of observed and modelled 1961–1990 average 1 April SWE (which is a benchmark for peak seasonal snow accumulation) between snow course sites (21 and 23 in the PR and UCR, respectively) and corresponding model pixels suggests some negative simulation bias but acceptable performance overall (Figure 3(a) and (b)). Nevertheless, discrepancies between individual observed and simulated SWE values are apparent, which are attributed to a combination of model error as well as to the effects of scale mismatch and possible lack of representativeness between snow course sites and model pixels (Andreadis and Lettenmaier 2006). Regardless, VIC-modelled 1 April SWE generally captures the regional variation of SWE with elevation in both the PR and UCR (Figure 3(c) and (d)).

Spatially distributed streamflow calibration was subsequently completed by subdividing the PR, UCR and CR study areas into 23, 24 and 1 sub-basins, respectively, based on Water Survey of Canada hydrometric stations and BC Hydro project sites. A set of five parameters were chosen on the basis of successful calibration in similar snowmelt-dominated environments in BC (Schnorbus *et al*., 2010) as well as previous sensitivity analysis (e.g. Demaria *et al*., 2007). A precipitation adjustment factor, *Padj*, is also included to accommodate bias in the historical precipitation data and hence bias in the downscaled precipitation data (Schnorbus *et al*., 2010). Biases are a result of interpolating from a sparse climate network weighted towards lower elevations (Adam *et al*., 2006; Stahl *et al*., 2006) and precipitation undercatch, particularly for solid precipitation (Adam and Lettenmaier 2003), which would tend to be more pronounced at high elevation stations where more precipitation falls as snow. Consequently, the application of precipitation bias correction factors is a common feature of hydrology models applied to the mountainous topography of BC (e.g. Quick, 1995; Stahl *et al*., 2008).

The VIC model simulated discharges were calibrated using the Multi-Objective Complex Evolution Method (Yapo *et al*., 1998). Three objective functions, the Nash–Sutcliffe coefficient of efficiency (NSE), NSE of log-transformed discharge (LNSE) and water balance error (WBE) were considered. The NSE provides a measure of overall 'goodness of fit', with higher values (closer to 1) indicating better agreement, whereas the LNSE provides a better criterion for the consideration of low flows. The WBE represents the ratio of the difference between cumulative observed and simulated discharges to the cumulative observed discharges, with values closer to zero indicating better agreement. The Pareto solutions from the multi-objective optimization provide trade-offs between the objective functions, and the optimum solution was subjectively chosen so as to balance NSE and LNSE, while keeping WBE within ±10%. All objective functions were calculated using daily discharge. Six years (1990–1995) of observed discharge (naturalized discharge for regulated sites) was used for model calibration, which is the period of highest streamflow data density in all three study areas (i.e. largest number of hydrometric stations with complete and overlapping records). An independent 5-year period (1985–1989)

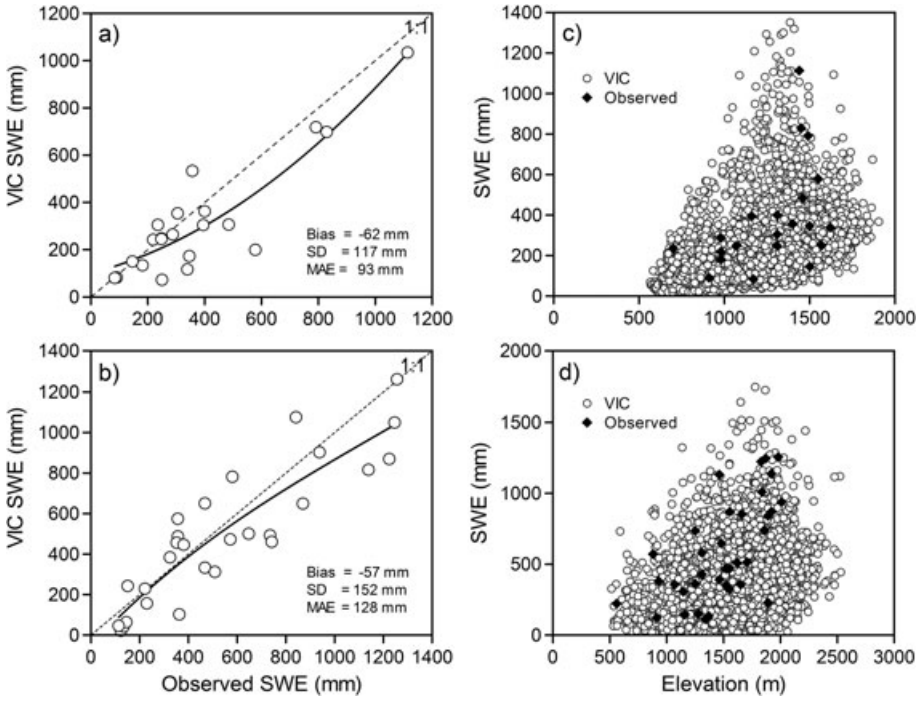

Figure 3. Comparison of observed and simulated 1961–1990 average 1 April snow water equivalent. Observed (snow course stations) and corresponding grid cell modelled SWE values are shown for the (a) PR and (b) UCR with trend lines estimated using local polynomial regression. Observed (snow course stations) and modelled (all grid cells) SWE values are plotted against elevation (station elevation for observed and grid cell elevation for modelled SWE) for the (c) PR and (d) UCR

was used for model validation. The 6-year calibration period is assumed to contain sufficient intra-annual and seasonal variability that parameter estimates will be robust to high frequency variability. However, low frequency, inter-annual and decadal climate variability, such as ENSO or PDO, is also known to strongly influence hydro-climatology in BC (Moore and McKendry, 1996; Romolo *et al.*, 2006; Fleming *et al.*, 2007), although the effects are spatially variable across the province (Fleming and Whitfield, 2010). The calibration period does not represent the full ENSO range, being dominated by warm episodes through 1991/1992 and 1994/1995 and neutral conditions in the remainder of the period, on the basis of the Oceanic Niño Index (Climate Prediction Center, 2010). The validation period contains both cold (1984/1985 and 1988/1989) and warm (1986/1987) ENSO episodes. Both the calibration and validation periods were dominated by the warm phase of the PDO (JISAO 2010).

Daily streamflow calibration and validation results for the three example study sites, BD, MD and SD, are given in Table III. Model performance is deemed good, with NSE and LNSE values >0.7 in most instances and WBE $<\pm 10\%$ in all but one occurrence. At all three sites, the chosen calibration appears quite robust, with little, if any degradation in performance between the calibration and validation periods. One exception is that performance does degrades with respect to WBE for the BD site (WBE $= -0.11$ during validation). This suggests overfitting of the *Padj* parameter to precipitation biases that prevailed during warm phase ENSO conditions, which does not accommodate the switch to more frequent wet type synoptic events that likely dominated the region during cold phase ENSO conditions of the validation period (Romolo *et al.*, 2006).

As additional validation, 30-year streamflow climatology simulated using both observed and downscaled climate data is compared with observed streamflow in Figure 4. Because of constraints in the observed streamflow data, comparison is based on the 1971–2000 period as opposed to 1961–1990. Bias is apparent in the modelled hydrographs at all three locations and is particularly high for the SD site during the fall and winter months. Discrepancies between observed streamflow and streamflow simulated with observed forcings are due to errors in the VIC model structure, VIC model parameters and inaccuracies in the forcing data, issues that appear more problematic when simulating fall–winter rainfall-generated runoff in the small coastal SD site. Despite bias correction with BCSD, using the downscaled climate data still introduces some additional bias to the simulated streamflow at all three locations. Discrepancies in the modelled discharge may also be due to errors in the observed streamflow data and, as is the case for the BD, MD and SD sites, naturalization of streamflow to remove the effects of storage and, in the case of SD, diversion. Because of the presence of simulation bias, changes in streamflow (and other fluxes) are quantified on the basis of comparison between simulated historical and future streamflows, rather than direct comparison with historical observations. Despite these errors, the annual cycle of monthly streamflow is well reproduced in all three examples. As such, we consider the hydrologic simulations to be sufficiently accurate for projecting the effects of climate change on a monthly, seasonal and annual basis.

Table III. Streamflow calibration and validation results for the BD, MD and SD sites

Study sites	Calibration			Validation		
	NSE	LNSE	WBE	NSE	LNSE	WBE
BD	0.64	0.84	0.01	0.75	0.86	−0.11
MD	0.89	0.83	−0.09	0.88	0.79	−0.07
SD	0.72	0.67	0.02	0.72	0.68	0.06

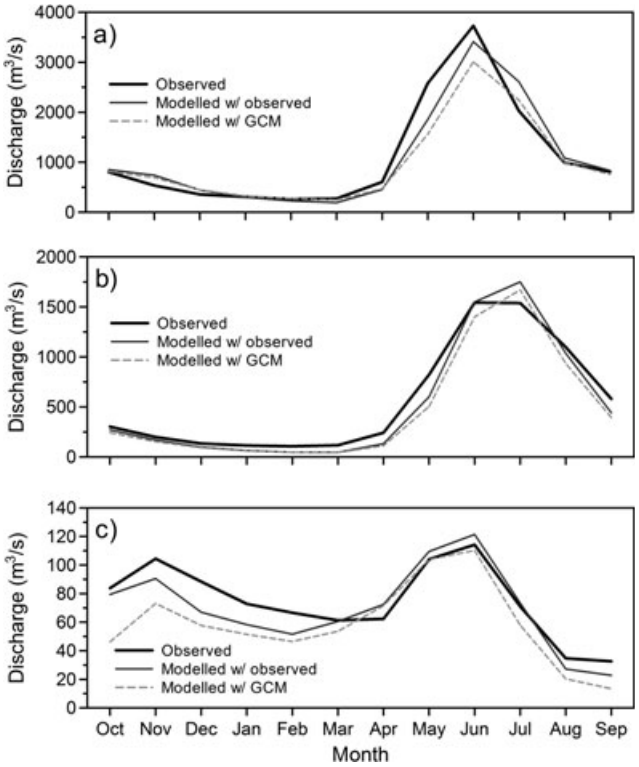

Figure 4. Comparison of observed (i.e. naturalized) and modelled (with either observed or downscaled GCM forcings) monthly average streamflows for the climatological period 1971–2000 for (a) BD, (b) MD and (c) SD. Modelled hydrographs using downscaled GCM forcings are shown as the median of the eight historical runs

The sensitivity of the simple glacier scheme is assessed by comparing simulated discharge for the period 1955–2006 for the MD site by using VIC runs (forced with observed climate data) both with and without glaciers initialized. Results are given in Figure 5, which shows monthly average discharge for August and September. Inclusion of glaciers increases August discharge on average by 16%, but the effect varies annually and ranges from $<1\%$ to 58%. In September, the relative effect is smaller, averaging only 10% and ranging from $<1\%$ to 34%. On an annual basis, glacier melt contributes an average of 3% of the discharge, varying between 0% and 12%. In the absence of a direct validation, we compare results with the recent work of Jost *et al.* (2011), which examined the contribution of glacier runoff to streamflow in the Mica basin by using a more

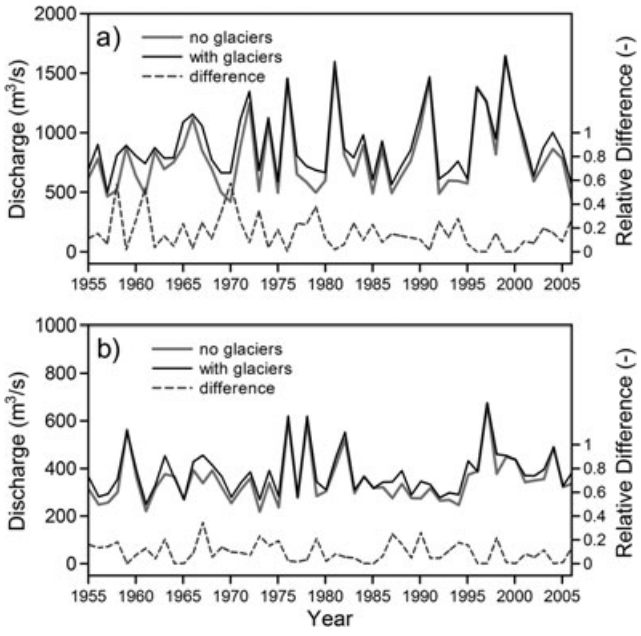

Figure 5. Effect of glaciers on mean monthly discharge at the MD site for (a) August and (b) September, which is shown by comparing discharge between VIC simulations initialized with and without glaciers

explicit glacier mass balance approach. The distinguishing features of the approach of Jost *et al.* (2011) are (1) a distinction between seasonal snowmelt and glacier ice melt, specifically the adoption of separate albedo values for snow and ice, and (2) calibration of the hydrologic model using observations of glacier retreat and volume loss. Our results for August compare favourably, but the September and annual glacier contributions are only half those simulated by Jost *et al.* (2011). Further, our results display higher inter-annual variability. This comparison suggests that using excess snow water as a simple proxy for glacier mass (*vs* explicitly modelling ice melt) potentially underestimates the magnitude of glacier melt in early fall and overestimates inter-annual variability. Although we consider our approach qualitatively effective, this comparison nevertheless suggests adopting a cautious approach with respect to interpreting the glacier response to climate change.

RESULTS AND DISCUSSION

Climate changes

The projected change in climate for all three study areas is shown in Figure 6 as temperature and precipitation changes for the 2050s period. The projections indicate a robust signal of increasing temperature in all three study areas for all three emission scenarios and all seasons. In all study areas, the A1B and B1 scenarios generate the greatest and least warming, respectively, by mid-century. It is noted that although the A2 scenario prescribes the greatest radiative forcing by the end of the century, the A1B scenario prescribes a greater radiative forcing by mid-21st century. Nevertheless, in most cases, the range of temperature projections overlaps considerably between emission scenarios.

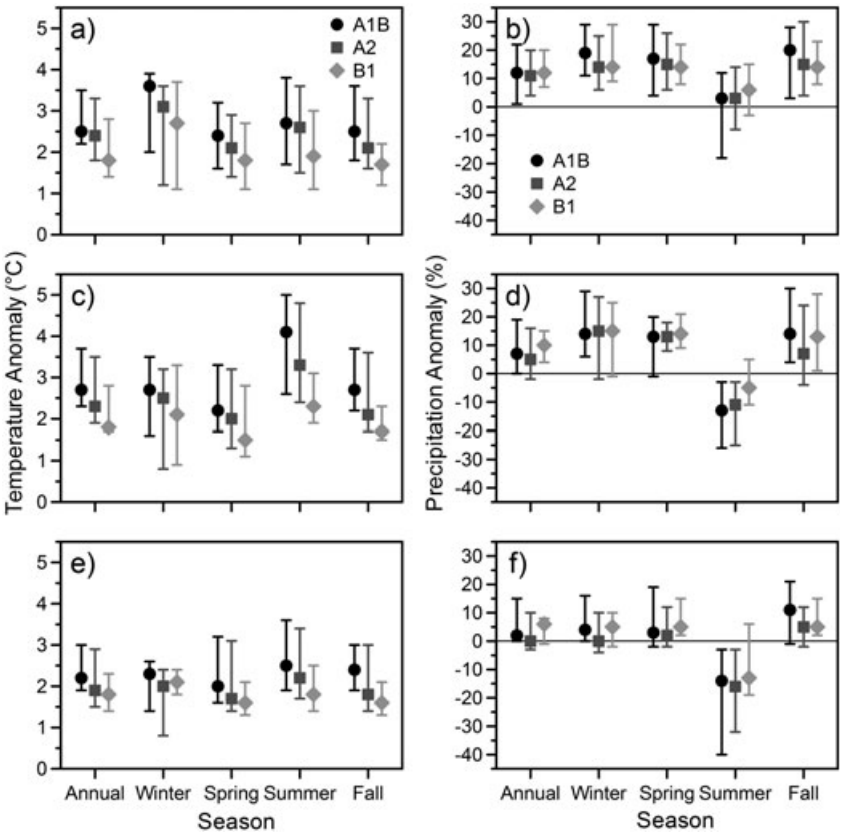

Figure 6. Projected 2050s climate changes for Peace (a) temperature and (b) precipitation, Upper Columbia (c) temperature and (d) precipitation, and Campbell (e) temperature and (f) precipitation. Individual plots show median change (symbols) with minimum to maximum range (lines)

For the PR in northern BC, projections consistently show increased precipitation during winter, spring and fall (Figure 6(b)). Winter, spring and fall precipitation projections are somewhat less consistent in southern BC, both in the UCR and more so in the coastal CR (Figure 6(d) and (f)), ranging from marginally drier to substantially wetter. Projected changes in summer precipitation are ambiguous in the PR, with median changes within ±5%, split roughly evenly between wetter and drier conditions for the A1B and A2 scenarios but weighted towards wetter conditions for the B1 scenario. In the UCR and CR, projections indicate a robust signal of decreasing summer precipitation for the A1B and A2 scenarios and range between wetter and drier conditions for the B1 scenario.

Snow

Given the importance of snow to the hydrologic regime in all three study areas, our discussion begins with a focus on projected seasonal snowpack changes. Such changes are analysed using two index variables. The first is the ratio of peak (i.e. 1 April) SWE to total cool season precipitation (October–March), *SWEp/Pw*, which is used to assess the effects of temperature changes on the relative contribution of snow storage within the hydrologic cycle (Barnett *et al.*, 2008). Nival (snow-dominated) regimes are classified as those where $SWEp/Pw \geq 0.5$, whereas hybrid regimes have values from ≥ 0.1 to <0.5, and pluvial (rainfall) regimes have ratios <0.1 (Elsner *et al.* 2010). The second index directly compares relative changes in *SWEp* between the historic and future periods and is a function of both temperature and precipitation changes. In the interest of brevity, the discussion that follows focuses on results primarily for the A1B scenario, which exhibits the highest warming at mid-century (although results for A2 and B1 are qualitatively similar). The median value is used as the consensus estimate for summarizing and comparing ensemble-based projection results.

Projected changes in *SWEp/Pw* generally indicate that with future warming, all three areas will transition to a regime less dominated by snow in the 2050s; however, regional and local variability is evident (Figure 7). In the PR, 30% of the study area, located mainly in the higher-elevation headwater regions in the northwest, is projected to remain snow dominated into the 2050s, although this represents a decrease from historical climate conditions, when half the study area is snow dominated. The lower-elevation southwestern and eastern portions of the PR are projected to transition to a more hybrid snow–rain-dominated (increasing from 49% to 58% of the area) or rainfall-dominated (increasing from 1% to 12% of the area) regime. In the historic period, most of the UCR experiences the majority of winter precipitation as snow (78% of the area), and the extent of rainfall-dominated winter precipitation is minimal (3% of the area). In the 2050s, there is a projected decline in overall *SWEp/Pw* over the UCR, and the area of rainfall and hybrid rain–snow is projected to increase in the 2050s (from 3% to 9% and form 19% to 31%, respectively). Nevertheless, roughly 60% of the UCR study area is at high enough elevation where the majority of winter precipitation

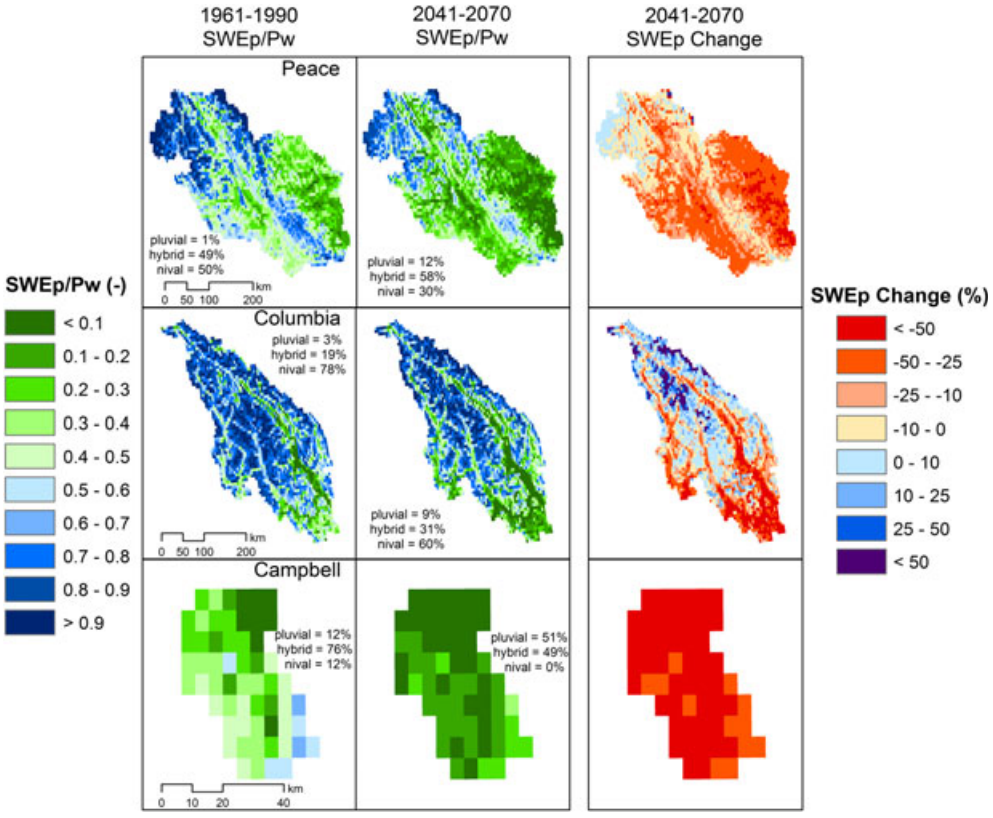

Figure 7. Snow storage in the PR, UCR and CR study areas, given as the ratio of 1 April *SWE* to winter precipitation (October–March) for the 1970s and 2050s and as the 2050s 1 April *SWE* change. All values are A1B scenario ensemble medians. SWE changes are given as seasonal values (i.e. absent the effect of glaciers)

will continue to fall as snow (Figure 7). In the CR, where baseline winter temperatures are near the freezing level, much of the basin already exhibits a rainfall-dominant or hybrid precipitation regime (12% and 76% of the area, respectively; Figure 7). In the 2050s, *SWEp*/*Pw* values are projected to change substantially, where roughly half of the CR study area will be entirely rainfall dominated, and snow-dominated areas will disappear entirely.

Basin-aggregated *SWEp* in the PR is projected to decrease by the 2050s (Table IV). This reflects the occurrence of decreased *SWEp* throughout most of the PR, with the exception of the northwest corner of the study area (Figure 7). Total *SWEp* in the UCR is projected to decrease (Table IV) by similar amounts for the A1B and A2 scenarios, and *SWEp* changes are projected to be marginal for the cooler B1 scenario. Spatially, the relative change in *SWEp* in the 2050s in UCR shows a strong relationship with temperature and thus elevation (Figure 7); changes are negative at low elevation (higher temperatures), tending to increase to positive changes with increasing elevation (and decreasing temperature). For the CR, overall *SWEp* is projected to decrease substantially in the 2050s for all three emission scenarios (Table IV). The median grid cell *SWEp* changes for the A1B scenario show a decrease in *SWEp* that is consistent across the entire study area (Figure 7). Despite this dramatic snow reduction, the sheer volume of precipitation experienced in the CR ensures that, even under increasingly rainfall-dominated conditions, snow will not be entirely lost and basin-average *SWEp* values on the order of 284–365 mm are projected for mid-century (which is still more snow than is simulated to accumulate throughout the drier PR during the historical period; Table IV).

Changes in snow accumulation generally respond most strongly to warming, which in most cases dominates over the response to increased fall and winter precipitation. Thus, basin-aggregated snow is projected to decline in all three study areas. Further, the magnitude of projected reductions in snow accumulation tends to reflect the magnitude of projected fall and winter warming, being highest and lowest for the A1B and B1 emission scenarios, respectively, particularly in the PR and UCR study areas (Figure 6). This finding is in agreement with previous studies in western North America, where observed snowpack changes over the 20th century are largely driven by temperature trends (Hamlet *et al*., 2005; Mote *et al*., 2005). Also, the greatest sensitivity of snow accumulation and melt to warming will occur in regions, such as the CR, where winter temperatures are already near freezing (Whitfield *et al*., 2002; Adam *et al*., 2009; Elsner *et al*., 2010). Nevertheless, because of the complex topography, strong local variation in the snow response is apparent. Figure 8, which compares monthly seasonal SWE change by elevation bands for the 2050s A1B scenario for both the PR and UCR, shows that projected snowpack change is negatively correlated with elevation (and, hence, temperature). At sufficiently high elevations, temperature does not increase enough mid-century to affect snow accumulation, such that local snowpack change is decoupled from the effect of widespread regional warming and exhibits greater sensitivity to projections of increasing winter precipitation, which is consistent with the other studies in the Pacific Northwest (Elsner *et al*., 2010). Consequently, the spatial variability of projected SWE change is affected by the elevation distribution within any given region (i.e. compare Figure 8 (a) and (b)). For instance, in the PR spring, SWE is projected to increase on the order of 10–20 mm above an approximate elevation of 1600 m (on the basis of grid cell average elevations); however, this accounts for only ~15% of the basin's area. This elevation threshold is roughly similar in south-eastern BC; however in the UCR, over 50% of the basin lies above 1600 m elevation, resulting in increased spring SWE over a much larger area with projected increases as high as 300 mm at the highest elevations.

Table IV. Summary of projected 2050s snow water equivalent changes by study area

Median peak SWE	Peace	Columbia	Campbell
61–90 (mm)	234	402	811
A1B change (%)	−23	−8	−65
A2 change (%)	−22	−7	−62
B1 change (%)	−11	1	−55

Runoff

Seasonal runoff changes are summarized in Table V, with seasons now defined as winter (December, January and February), spring (March, April and May), summer (June, July and August) and fall (September, October and November). The median is used to estimate the consensus response by study area and emission scenario. Some regional variation in runoff response is apparent. Projected runoff changes are of the same relative order in all three areas in the winter and fall (although much larger in the CR in absolute terms), being substantially larger in winter. In the spring, large relative increases in runoff are projected for the PR and UCR, whereas projected increases for the CR are smaller by an order of magnitude. Summer runoff is projected to decrease in all three areas, but relative decreases are substantially larger in the coastal CR as compared with the interior PR and UCR areas. Differences in runoff changes between emission scenarios vary by season and by area, with no consistency as to which scenarios produce the largest or smallest changes.

The seasonal runoff changes generally reflect the changes in precipitation and snow storage already discussed. As an example, the spatial distribution of spring and summer seasonal runoff changes is shown in Figure 9 for the A1B ensemble median. Spatially, spring runoff changes are generally positively correlated with the projected *SWEp* changes (cf. Figure 7), suggesting increased total snowmelt runoff from areas that will

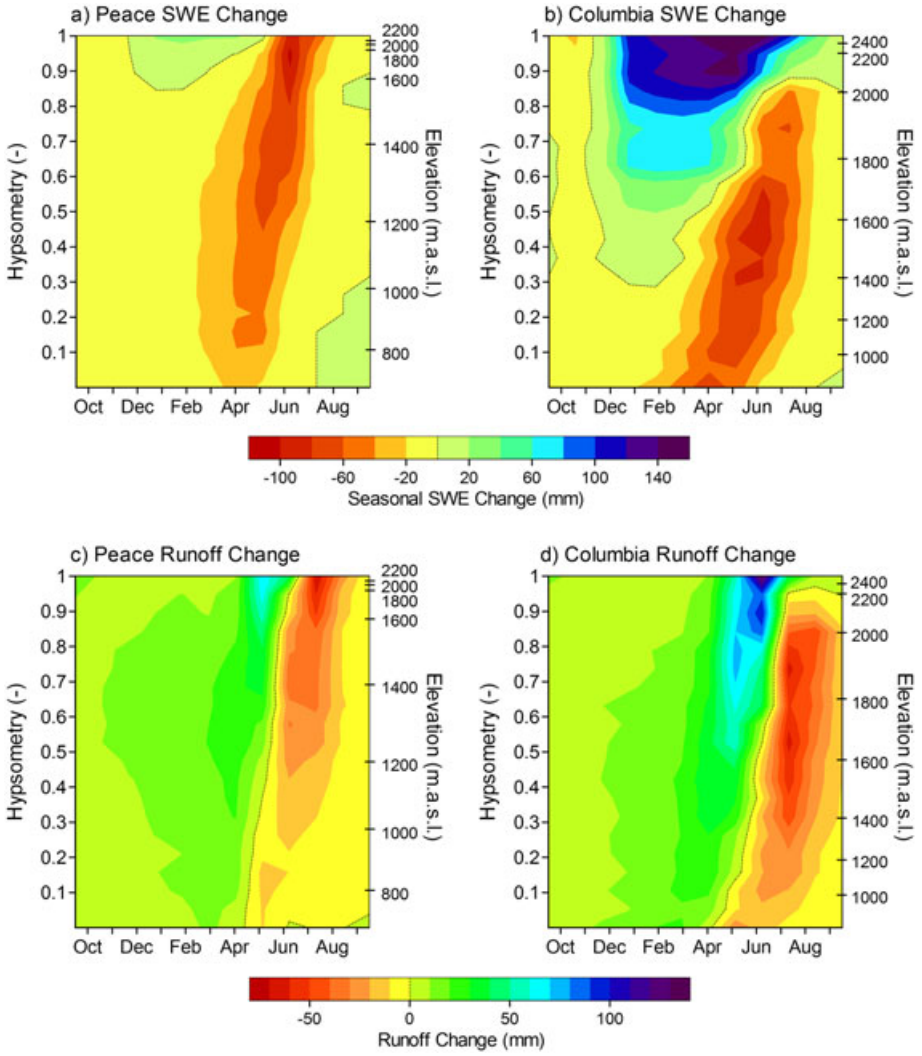

Figure 8. Contour plot of monthly SWE change by elevation in the (a) PR and (b) UCR and monthly runoff change by elevation in the (c) PR and (d) UCR for the A1B scenario ensemble median. Note that elevation is given as a percentile of the basin hypsometric curve on the primary *y*-axis (elevation above sea level is given on the secondary *y*-axis). SWE changes are given as seasonal values (i.e. absent the effect of glaciers)

Table V. Summary of projected 2050s runoff changes

Median runoff	Annual	Winter (DJF)	Spring (MAM)	Summer (JJA)	Fall (SON)
Peace River (PR)					
61–90 (mm/period)	414	40	105	195	74
A1B change (%)	11	77	56	−25	8
A2 change (%)	10	67	53	−22	4
B1 change (%)	12	55	45	−13	7
Upper Columbia River (UCR)					
61–90 (mm/period)	682	31	140	428	83
A1B change (%)	7	95	77	−22	5
A2 change (%)	10	98	79	−16	−1
B1 change (%)	9	75	52	−9	8
Campbell River (CR)					
61–90 (mm/period)	2348	560	685	604	500
A1B change (%)	2	55	5	−58	11
A2 change (%)	1	46	4	−52	7
B1 change (%)	3	45	8	−45	5

experience future increases in snow storage. Consequently, spring runoff is projected to increase with increasing elevation, particularly in the UCR (Figure 8). At low elevation, spring runoff changes are negative. In the summer, the median A1B 2050s runoff changes are negative throughout most of the PR, UCR and CR. The

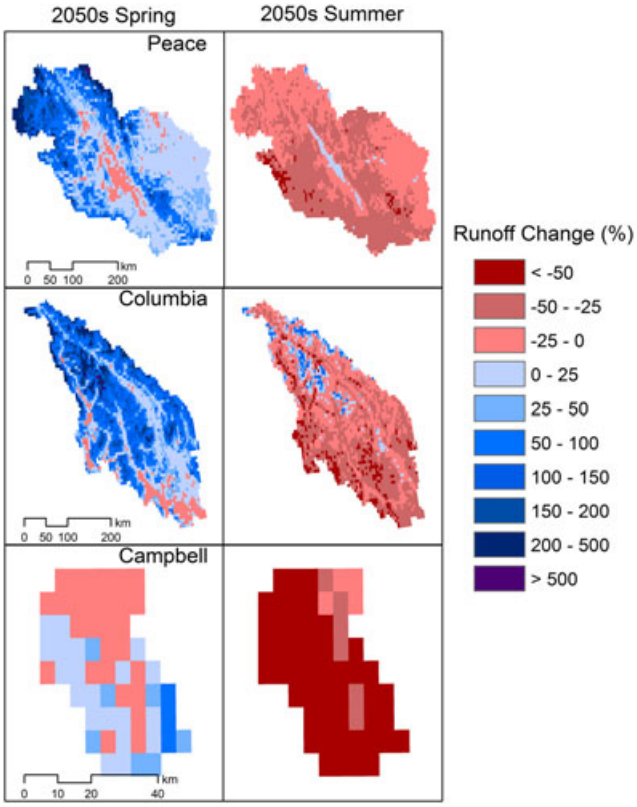

Figure 9. Median A1B 2050s spring and summer runoff changes for the PR, UCR and CR study areas

exception is the occurrence of positive runoff changes from high-elevation areas in the northern portion of the UCR study area (see also Figure 8). Although the simple glacier scheme does not explicitly discriminate between seasonal snowmelt and glacier melt (both are lumped as snowmelt), the location of the summer runoff increases coincides with locations of mid-21st century perennial snow and ice (not shown), suggesting that the increased runoff derives from increased glacier melt (see Section on Glacier Response). Conversely, runoff changes are negative in those grid cells in which glaciers (i.e. perennial snow) disappear in the 2050s. The fall season is characterized by minimal snow cover, and fall runoff changes, which reflect changes in the balance between rainfall, evapotranspiration, glacier melt and soil moisture (not shown), tend to exhibit little overall correlation with elevation (Figure 8).

On an annual basis, runoff is projected to increase in the two interior areas by the same relative amount but remain unchanged in the coastal area. These annual runoff changes primarily reflect projected changes in annual precipitation in the PR and CR, as well as the loss of glacier storage in the UCR. Figure 10 shows the change in annual precipitation and runoff by elevation in the PR and UCR study areas for the A1B scenario. In the PR, the changes in precipitation and runoff with elevation are essentially identical trends, although precipitation changes are larger than runoff changes because of increasing evaporation (Figure 10(a)). In the UCR, the changes in precipitation and runoff below approximately 1600 m elevation (based on grid-cell average elevations) are similar to those in the PR. However, above 1600 m elevation, the change in runoff shows a much steeper trend with elevation such that above 2000 m (approximately 20% of the area) projected changes in annual runoff greatly exceed those of precipitation (Figure 10 (b)), suggesting that increased runoff is derived from decreasing glacier storage. It is acknowledged, however, that the degree to which annual runoff in the UCR is affected by changes in glacier storage is the subject of some uncertainty (see Section on Glacier Response).

Glacier response

Figure 11 shows the simulated glacier mass balance averaged over the UCR study area, divided into positive (accumulation), negative (ablation) and net balance, with results given for the A1B ensemble median. Given the longer response time of glaciers, projected results are depicted not only for mid-21st century (2041–2070) but also for the near-term (2011–2040) and long-term (2070–2098). Results show that net mass balance is

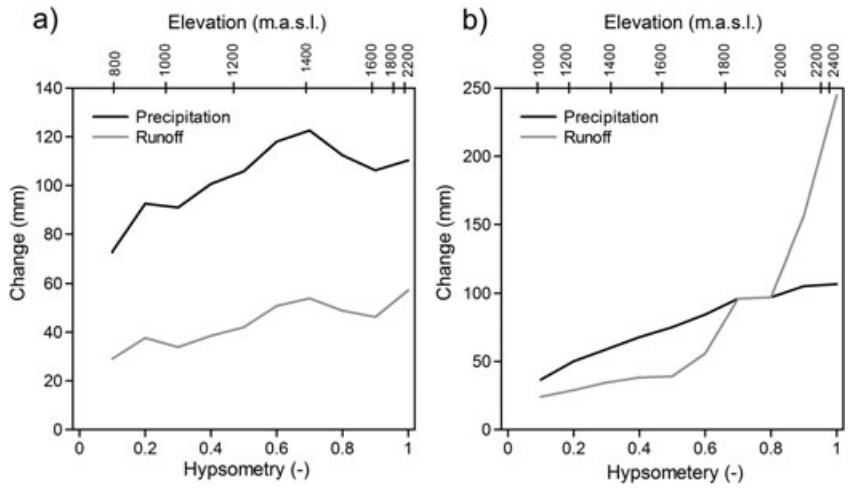

Figure 10. Median A1B annual runoff change by grid-cell elevation in the (a) PR and (b) UCR. Runoff change is averaged over ten elevation bands of equal area, where elevation is given as a percentile of the basin hypsometric curve on the primary *x*-axis (elevation above sea level is given on the secondary *x*-axis)

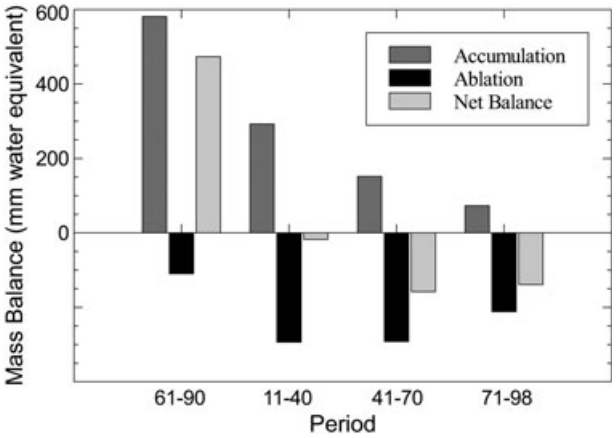

Figure 11. Median A1B specific glacier mass balance for the UCR averaged over the historic period (1961–1990) and three future periods (2011–2040, 2041–2070 and 2071–2098)

projected to be positive during 1961–1990 and, consistent with rising temperatures, negative in all three future periods. However, the historic mass balance results are inconsistent with observations that show that the historical period is already characterized by negative glacier mass balance in south-eastern BC, which has led to a decline in glacier area and volume (Debeer and Sharp, 2007; Schiefer *et al.*, 2007). Although a period of elevated melt and runoff volume typically follows a transition from near-neutral to negative glacier mass balance, a prolonged period of negative mass balance will eventually result in glacier retreat and a resultant decline in glacier runoff volume (Hock *et al.*, 2005). Consistent with observations of glacier retreat, there has been an observed trend of declining August streamflow in glaciarized basins in southern BC (Stahl and Moore, 2006), suggesting that glaciers in the UCR have already passed the period of elevated runoff and are now in the declining phase in response to regional warming. This is again contrary to the simulation results, which suggest that glacier runoff in the UCR (interpreted as the negative balance in Figure 11) is projected to increase until mid-century and then decline slightly.

This discrepancy between simulated and observed mass balances is attributed to a number of factors. In reality, ice mass accumulating at high elevation would be dynamically redistributed to lower elevations where it would be subject to warmer temperatures (Smithson *et al.*, 2002). Neglecting glacier dynamics results in an unrealistic monotonic accumulation of ice mass in the accumulation area (Huss *et al.*, 2010) and an underestimate of ablation at lower elevations. Additionally, glacier melt is modelled using the standard albedo depletion curves for snow with the result that glacier albedo values may be overestimated and melt underestimated (Kaser *et al.*, 2006). In the current implementation, there is a likely tendency for simulated glaciers to retreat to a 'friendlier' climate at higher elevation where they build unchecked throughout the historic period, delaying the transition to negative mass balance by several decades. The use of a contemporary glacier state (i.e. *ca* 1995) to initialize the model likely also underestimates the volume of low-elevation glacier ice that would have been present in 1950, underestimating glacier ablation and biassing the estimate of net balance in the historic period. The net effect is that projected runoff from glacier melt is likely underestimated during the baseline period and overestimated for the 2050s (e.g. Stahl *et al.*, 2008), an issue that would most acutely affect late-summer and early-fall streamflow projections (e.g. August and September). However, this does not fundamentally change the conclusions for the summer period, other than to indicate that the projected decline in summer runoff may be too conservative. This issue does add some ambiguity to the fall runoff projections for the UCR, which currently show increased future runoff by the 2050s. To address these issues in future studies, we are currently working towards including a more realistic representation of glacier mass balance and dynamics in subsequent hydrologic projections in the UCR.

Study site response

Historical and projected monthly temperature, precipitation (including rainfall and snowfall), snowmelt and discharge are illustrated in Figures 12 and 13 for the BD

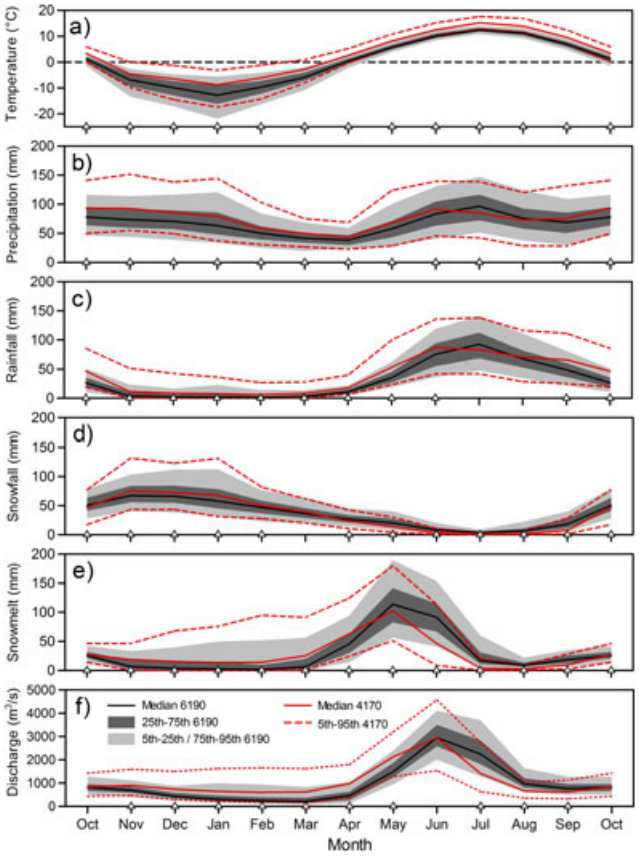

Figure 12. Comparison of historic (1961–1990) and future (2041–2070) monthly (a) temperature, (b) precipitation, (c) rainfall, (d) snowfall, (e) snowmelt and (f) discharge for the A1B ensemble for the drainage area upstream of the Peace River at Bennett Dam (BD). Historic values are represented by the median (solid black line), inter-quartile range (dark grey shading) and 5th and 95th percentiles (light grey shading). Future values are represented by the median (solid red line) and 5th and 95th percentiles (dotted red lines). Those months where the future ensemble differs significantly ($\alpha = 0.05$) from the historic are indicated by a triangle

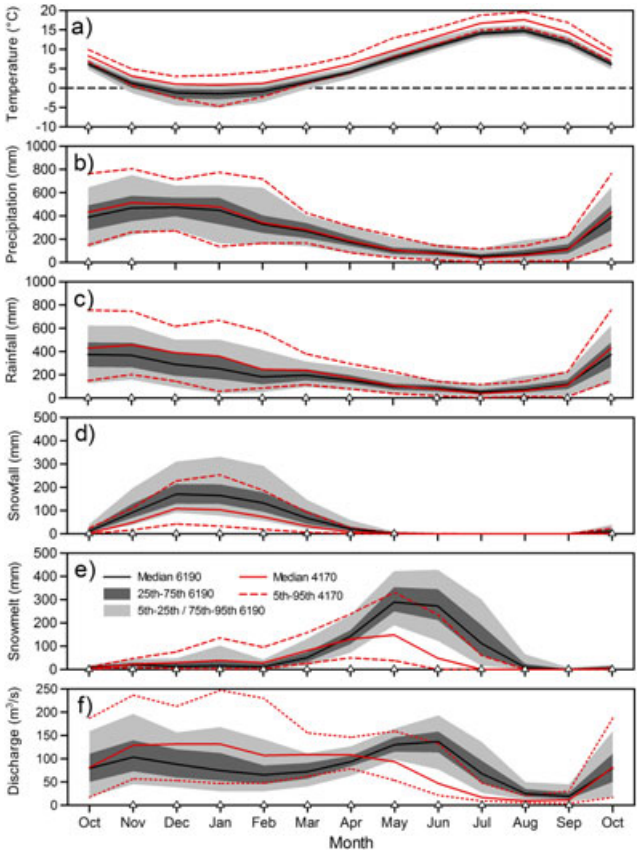

Figure 13. As per Figure 12, but for the drainage area upstream of the Campbell River at Strathcona Dam (SD)

and SD sub-basins, respectively. As results for MD are qualitatively similar to those of BD, they are not included. Individual plots show separate historical and future distributions of each monthly variable by using combined results from the A1B scenario ensemble (i.e. 8×30 values for each month in each period). The historical distribution of each variable is presumed to be predominantly a function of inter-annual variability because downscaling has corrected most aspects of GCM bias. The monthly ensemble distributions for the future period, however, reflect both potential changes in inter-annual variability as well as the variation (i.e. divergence) in individual GCM response to the A1B radiative forcing. Any historic and future monthly distributions that exhibit statistically significant differences (two-sided Wilcoxon rank-sum test, $\alpha = 0.05$, Helsel and Hirsch 2002) are denoted in Figure 12 and indicate significant changes by month with respect to both inter-annual and inter-GCM variability.

Warmer temperatures are projected throughout the year by mid-century for the area upstream of BD (Figure 12 (a)). Nevertheless, monthly average winter temperatures will remain below freezing. Increased future precipitation during fall and winter (Figure 12(b)) will manifest as increases in both rainfall and snowfall (Figure 12(c) and (d)). The BD sub-basin is also projected to experience increased snowmelt in winter, spring and early summer (Figure 12(e)), which is consistent with increasing temperatures. The decline in *SWEp*/*Pw* projected for mid-century (Figure 7) appears therefore to be not only a function of a strict change in precipitation phase (both snowfall and rainfall are projected to increase) but also a function of an increasingly transient winter snowpack. The shift to higher discharge during winter in the future correlates with increases in both snowmelt and rainfall. Changes in the timing and magnitude of the spring freshet (Figure 12(f)) result from increased spring rainfall and snowmelt (Figure 12(c) and (e)), followed by decreased snowmelt and discharge in the summer.

Following a shift to warmer temperatures in all months in the 2050s for SD, winter temperatures are projected to be predominantly above freezing (Figure 13). Statistically significant precipitation changes are only evident for the summer months of June, July and August (reduced precipitation) and the fall months of October and November (increased precipitation; Figure 13(b)). Although the reduction in median summer precipitation is projected to be relatively large (−14% for A1B; Figure 6), summer is the driest part of the year on the BC south coast, and the absolute projected precipitation change is negligible (Figure 13(b)). Rainfall is projected to increase and snowfall to decrease throughout the fall, winter and spring (Figure 13(c) and (d), respectively), and these respective changes are larger in magnitude (and statistically significant for a larger number of months) than those projected for precipitation. Therefore, increased rainfall is predominantly in response to a change in precipitation phase due to higher winter temperatures. This increased rainfall drives higher discharge in the fall and winter (Figure 13(f)). The earlier loss of snow storage (due to increased mid-winter melt and reduced snowfall) and raised evaporation (not shown) in the spring and summer results in a pronounced decrease in discharge during May–September. By mid-century, the discharge at SD is projected to change from a hybrid to a predominantly rainfall-dominated (pluvial) regime.

Figure 14 compares historic and future simulated monthly discharges for each individual projection. We use the median of each individual projection to focus on the variability of the projected streamflow response due to choice of emission scenario and GCM. Despite considerable variability between individual projections, there is a high degree of consistency in terms of the direction of projected streamflow changes. BD and MD will retain the traits of a nival regime (Figure 14(a) and (b)), but there is strong agreement for a shift to increased (decreased) discharge in the winter/spring (summer/early fall). For the MD site (with 8% glacier cover *ca* 1995), the decrease in streamflow projected for late summer/early fall, particularly August and September, may be underestimated as a result of a delayed glacier response in the VIC model. Consequently, the actual degree to which the MD site retains a glacier signature in the monthly hydrograph by the 2050s remains unclear. Individual streamflow projections for the SD site show strong agreement for a shift from a hybrid system to one that is predominantly pluvial, with increased (decreased) winter (summer) discharge projected by mid-century (Figure 14(c)). Variability in

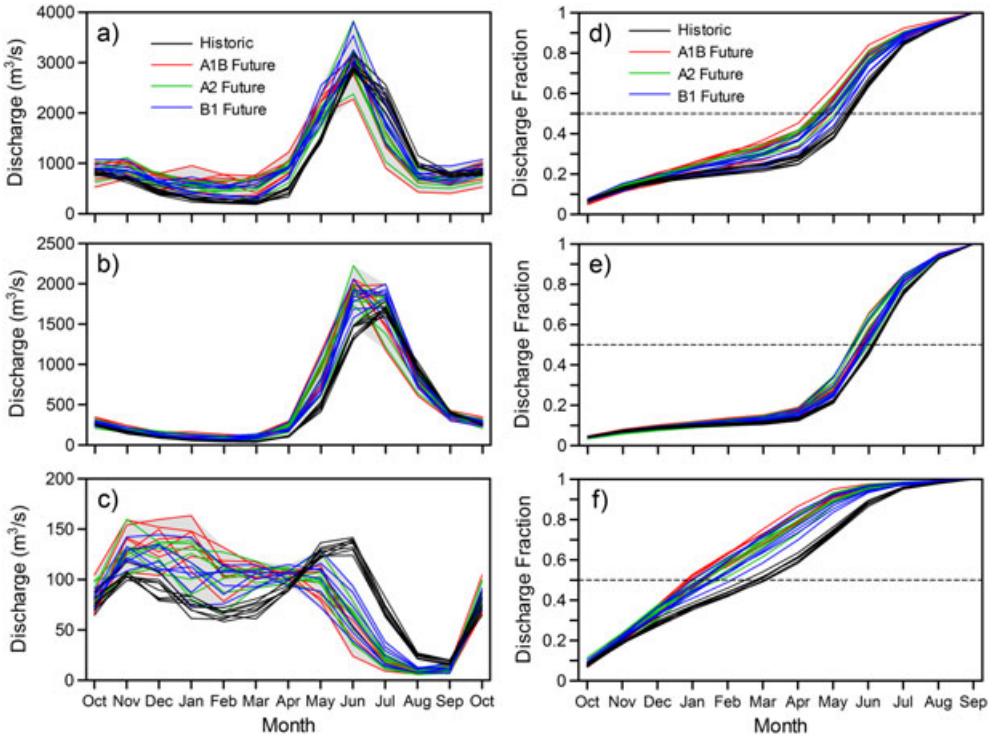

Figure 14. Monthly discharge for (a) the Peace River at Bennett Dam (BD), (b) Columbia River at Mica Dam (MD) and (c) Campbell River at Strathcona Dam (SD) and fraction of cumulative annual discharge for (d) BC, e) (MD and (f) SD. Historic (1961–1990; black lines) and future (2041–2070; coloured lines) discharge is given as the median monthly value from each individual GCM-driven projection, for a total of 8 and 23 unique historic and future values, respectively

projected streamflow during the fall and winter months is higher for the SD site than in either BD or MD site. This reflects differences in streamflow sensitivity to fall and winter rainfall changes between the colder interior study areas and the warmer, more temperate coastal study area. Despite increasing rainfall, the 2050s runoff in BD and MD is still strongly affected by the presence of snow storage and the occurrence of snowmelt, and streamflow at these locations is predominantly affected by variability in the temperature projections. In the 2050s, fall and winter runoff in the CR is increasingly rainfall dominated, such that streamflow changes are sensitive to variability between projections of both temperature and, more so than either BD or MD, precipitation.

Plots of normalized cumulative monthly discharge over the water year show a transition to earlier streamflow timing in all three study areas (Figure 14(d)–(f)). By using the half flow index (date of occurrence of 50% of the annual discharge; dotted line in Figure 14(d)–(f)), shifts in streamflow timing range from several days to over a month for BD, depending upon emission scenario and GCM. For the MD site, streamflow-timing shifts are smaller in magnitude (all less than 1 month) and less variable than at the BD site. The SD site exhibits the largest shift in streamflow timing (and the greatest variability), with individual shifts ranging from several weeks to over 2 months.

Projections of median monthly discharge for mid-century appear to be largely insensitive to the trajectory of the three selected emission scenarios. The Steel–Dwass multi-comparison test (Hollander and Wolfe 1999) was used to test for significant differences ($\alpha = 0.05$) between the A1B, A2 and B1 streamflow projection ensembles for each month. With one exception, results indicate that for all three study sites, there are no significant differences in any month between scenarios, such that streamflow projections under A1B, A2 and B1 can be considered statistically indistinguishable. A single exception occurs for the BD site, where A1B and B1 projections are significantly different ($p < 0.05$) in August.

The projected streamflow changes are generally robust (with respect to the selected emission trajectories and GCM variability) when compared with the simulated baseline conditions. However, given the presence of hydrologic modelling errors, in particular the biases shown in Figure 4, it is unclear to what degree the projected changes simulated by the VIC model represent a likely real-world streamflow response to the given climate perturbations. A simple assumption is that streamflow modelling bias is stationary throughout the projection timeframe. In the case of a constant additive bias, this means the change in simulated streamflow between future and baseline (ΔQ_s) would equal the real streamflow change (ΔQ_{real}), or $\Delta Q_{real} = \Delta Q_s$. In the case of multiplicative bias, $\Delta Q_{real} = \Delta Q_s / b$ (where the bias, b, is estimated as the ratio of simulated to observed average streamflow), the magnitude of the real changes would be either overestimated ($b > 1$) or underestimated ($b < 1$) by ΔQ_s. Therefore, the streamflow changes given in Figure 14 would generally reflect real changes, either because bias is additive or, in the case of multiplicative bias, the simulated changes would be a conservative

estimate of real changes (given the tendency to underestimate streamflow in Figure 4). However, one cannot necessarily assume that modelling bias remains constant under non-stationary climatic conditions, particularly in watersheds such as the CR where regime shifts potentially alter the dominant runoff mechanisms. In this case, the modelling uncertainty is currently unquantified. Nevertheless, as the hydrographs given in Figure 14 represent physically plausible responses of nival and hybrid nival–pluvial regimes to increasing temperature and changing precipitation, the simulated streamflow changes are considered a qualitatively robust indication of the real streamflow response to the assumed emission trajectories.

CONCLUSIONS

This study utilized a suite of eight GCMs driven by three emission scenarios to project a wide range of plausible climate responses for the 2050s period (2041–2070). The climate projections were statistically downscaled and used to drive the spatially distributed VIC hydrologic model at high resolution. The resultant hydrologic response was captured for three study areas in BC (the Peace, Campbell and Upper Columbia), reflecting variation in regional hydrologic response across a range of climatic and physiographic regimes. Streamflow projections were made for several project sites within the study areas; results from three sites are described here.

Downscaled climate projections show warming for the 2050s in all three study areas across all seasons, for all GCMs and emission scenarios. There is high level of consensus for increased precipitation in the fall, winter and spring months in the interior of BC (the PR and UCR study areas) for all three emission scenarios. In south-coastal BC (the CR), projections also suggest increased winter, spring and fall precipitation, although the level of consensus between individual projections is not as high. There is a high degree of consensus for a decrease in summer precipitation in southern BC (CR and UCR). Summer precipitation results for north-eastern BC (the PR) are more ambiguous.

By the 2050s, climate change will affect the hydrology of the Peace, Campbell and Upper Columbia watersheds to varying degrees. Predominantly in response to province-wide warming, SWE is projected to decline throughout the Peace and Campbell and at lower elevations in the Upper Columbia. At higher elevations in the Upper Columbia, where winter temperatures will still remain below freezing, snow water is projected to increase with increasing winter precipitation. In aggregate, snow water is projected to decline in all three basins, although reductions are projected to be greatest in the lower-elevation, warmer CR area and least in the high-elevation and colder interior UCR area. Runoff changes in the three areas vary spatially and seasonally and generally reflect snow and precipitation changes and topography-based temperature gradients. On an area-average basis, these changes generally include higher runoff in the winter and spring and reduced runoff in the summer. An unrealistically delayed glacier response to increasing temperature in the VIC model leads to some uncertainty in the summer and fall runoff projections for the UCR, although the conclusion of reduced summer runoff in this region remains robust.

Climate change is projected to affect streamflow timing in all three areas. The effect is most pronounced in the coastal Campbell system, where discharge at the SD site is expected to transition almost entirely to a pluvial system, with the winter season becoming the predominant discharge period. Changes in the interior Peace (BD site) and Upper Columbia (MD site) systems reflect a reduction in the influence of snow, including a shift to higher discharge in winter, an earlier freshet and reduced discharge in summer; however, discharge will still generally retain the characteristics of a nival regime. Differences in response between BD and MD (i.e. larger projected winter discharge increase in BD than MD) reflect hypsometric differences that result in higher sensitivity to temperature changes in the PR region affecting the BD site. The degree to which the MD site transitions from a glacial–nival regime to strictly nival regime by the mid-21st century is potentially underestimated in the current study. In general, projected trends of monthly and seasonal mid-century streamflow change at all three locations are robust with respect to the choice of GCM and emission scenario. Despite the errors inherent in the hydrologic modelling process, the hydrologic changes simulated within each study area are considered a physically plausible and qualitatively robust response to projections of increasing temperature and changing precipitation.

ACKNOWLEDGEMENTS

We acknowledge the financial support of BC Hydro, BC Ministry of Environment and Natural Resources Canada. This work benefited from discussions with the members of BC Hydro's Technical Advisory Committee (Alex Cannon, Alan Chapman, Sean Fleming, Doug McCollor, Brian Menounos, Dan Moore, Stephanie Smith and Frank Weber). We are also grateful for the constructive comments from two anonymous reviewers.

REFERENCES

Adam JC, Lettenmaier DP. 2003. Adjustment of global gridded precipitation for systematic bias. *Journal of Geophysical Research-Atmospheres* **108**(D9): DOI 10.1029/2002JD002499.

Adam JC, Clark EA, Lettenmaier DP, Wood EF. 2006. Correction of global precipitation products for orographic effects. *Journal of Climate* **19**(1): 15–38.

Adam JC, Hamlet AF, Lettenmaier DP. 2009. Implications of global climate change for snowmelt hydrology in the twenty-first century. *Hydrological Processes* **23**(7): 962–972.

Andreadis KM, Lettenmaier DP. 2006. Assimilating remotely sensed snow observations into a macroscale hydrology model. *Advances in Water Resources* **29**(6): 872–886, DOI 10.1016/j.advwatres.2005.08.004.

Annan JD, Hargreaves JC. 2010. Reliability of the CMIP3 ensemble. *Geophysical Research Letters* **37**, DOI 10.1029/2009GL041994.

Auer Jr AH. 1974. The rain versus snow threshold temperatures. *Weatherwise* **27**(2): 67.

Bahr DB, Meier MF, Peckham SD. 1997. The physical basis of glacier volume-area scaling. *Journal of Geophysical Research Solid Earth* **102**(B9): 20,355–20,362.

Barnett TP, Adam JC, Lettenmaier DP. 2005. Potential impacts of a warming climate on water availability in snow-dominated regions. *Nature* **438**(7066): 303–309.

Barnett TP, Pierce DW, Hidalgo HG, Bonfils C, Santer BD, Day T, Bala G, Wood AW, Nozawa T, Mirin AA, Cayan DR, Dettinger MD. 2008. Human-induced changes in the hydrology of the western United States. *Science* **319**(5866): 1080–1083.

Barry RG. 1992. *Mountain weather and climate*, 2nd edn. Routledge physical environment series: Routledge, London, UK and New York, NY.

Bartlett PA, MacKay MD, Verseghy DL. 2006. Modified snow algorithms in the Canadian land surface scheme: model runs and sensitivity analysis at three boreal forest stands. *Atmos Ocean* **44**(3): 207–222.

Batjes N. 1995. A homogenized soil data file for global environmental research: a subset of FAO, ISRIC and NRCS profiles (Version 1.0). Working Paper and Preprint 95/10b, International Soil Reference and Information Centre, Wagenigen, The Netherlands

BC Integrated Land Management Bureau. 1995. Baseline thematic mapping, release 1.0.

Bennett KE, Werner AT, Schnorbus MA. 2012. Uncertainties in hydrologic and climate change impact analyses in headwater basins of British Columbia. *Journal of Climate* **25**(17): 5711–5730, DOI: 10.1175/JCLI-D-11-00417.1

Blöschl G, Montanari A. 2010. Climate change impacts-throwing the dice? *Hydrological Processes* **24**(3): 374–381.

Bonfils C, Santer BD, Pierce DW, Hidalgo HG, Bala G, Das T, Barnett TP, Cayan DR, Doutriaux C, Wood AW, Mirin A, Nozawa T. 2008. Detection and attribution of temperature changes in the mountainous western United States. *Journal of Climate* **21**(23): 6404–6424.

Bras RL. 1990. *Hydrology: An Introduction to Hydrologic Science*. Addison-Wesley Publishing Company: Reading, MA.

Bürger G, Schulla J, Werner AT. 2011. Estimates of future flow, including extremes, of the Columbia River headwaters. *Water Resources Research* **47**: W10520, DOI: 10.1029/2010WR009716

Campbell GS, Norman JM. 1998. *An introduction to environmental biophysics*, 2nd edn. Springer: New York, NY.

Carroll A, Regniere J, Logan J, Taylor S, Bentz B, Powell J. 2006. Impacts of climate change on range expansion by mountain pine beetle. Mountain Pine Beetle Initiative Working Paper 2006–14, Natural Resources Canada, Canadian Forest Service, Pacific Forestry Centre, Victoria, BC.

Chang H, Jung I. 2010. Spatial and temporal changes in runoff caused by climate change in a complex large river basin in Oregon. *Journal of Hydrology* **388**(3–4): 186–207, DOI: 10.1016/j.jhydrol.2010.04.040

Christensen NS, Wood AW, Voisin N, Lettenmaier DP, Palmer RN. 2004. The effects of climate change on the hydrology and water resources of the Colorado River Basin. *Climate Change* **62**(1–3): 337–363.

Climate Prediction Center. 2010. Historical el nino/la nina episodes (1950-present). URL http://www.cpc.ncep.noaa.gov/products/analysis_monitoring/ ensostuff/ensoyears.shtml, last accessed 2 December, 2010.

Cohen SJ, Miller KA, Hamlet AF, Avis W. 2000. Climate change and resource management in the Columbia River basin. *Water International* **25**(2): 253–272.

Collins WD, Bitz CM, Blackmon ML, Bonan GB, Bretherton CS, Carton JA, Chang P, Doney SC, Hack JJ, Henderson TB, Kiehl JT, Large WG, McKenna DS, Santer BD, Smith RD. 2006. The community climate system model version 3 (CCSM3). *Journal of Climate* **19**: 2122–2143, DOI: 10.1175/JCLI3761.1

Collins M, Tett SFB, Cooper C. 2001. The internal climate variability of HadCM3, a version of the Hadley Centre coupled model without flux adjustments. *Climate Dynamics* **17**: 61–81, DOI: 10.1007/s003820000094

Daly C, Neilson RP, Phillips DL. 1994. A statistical topographic model for mapping climatological precipitation over mountainous terrain. *Journal of Applied Meteorology* **33**(2): 140–158.

Debeer CM, Sharp MJ. 2007 .Recent changes in glacier area and volume within the southern Canadian Cordillera. *Annals of Glaciology* **46**(1): 215–221, DOI: 10.3189/172756407782871710

Delworth TL, Broccoli AJ, Rosati A, Stouffer RJ, Balaji V, Beesley JA, Cooke WF, Dixon KW, Dunne J, Dunne KA, Durachta JW, Findell KL, Ginoux P, Gnanadesikan A, Gordon CT, Griffies SM, Gudgel R, Harrison MJ, Held IM, Hemler RS, Horowitz LW, Klein SA, Knutson TR, Kushner PJ, Langenhorst AR, Lee H, Lin S, Lu J, Malyshev SL, Milly PCD, Ramaswamy V, Russell J, Schwarzkopf MD, Shevliakova E, Sirutis JJ, Spelman MJ, Stern WF, Winton M, Wittenberg AT, Wyman B, Zeng F, Zhang R. 2006. GFDL's CM2 global coupled climate models. Part I: formulation and simulation characteristics. *Journal of Climate* **19**: 643–674, DOI: 10.1175/JCLI3629.1

Demarchi DA. 1996. An introduction to the ecoregions of British Columbia. URL http://www.env.gov.bc.ca/ecology/ecoregions/title_author.html,last accesed 18 August 2010.

Demaria EM, Nijssen B, Wagener T. 2007. Monte Carlo sensitivity analysis of land surface parameters using the Variable Infiltration Capacity model. *Journal of Geophysical Research-Atmospheres* **112**(D11).

Déry SJ, Stahl K, Moore RD, Whitfield PH, Menounos B, Burford JE. 2009. Detection of runoff timing changes in pluvial, nival, and glacial rivers of western Canada. *Water Resources Research* **45**, DOI: 10.1029/2008WR006975

Dickinson RE, Henderson-Sellers A, Rosenzweig C, Sellers PJ. 1991. Evapotranspiration models with canopy resistance for use in climate models – a review. *Agricultural and Forest Meteorology* **54**(2–4): 373–388.

Ducoudré NI, Laval K, Perrier A. 1993. SECHIBA, a new set of parameterizations of the hydrologic exchanges at the land atmosphere interface within the LMD atmospheric general-circulation model. *Journal of Climate* **6**(2): 248–273.

Dyurgerov M, Meier M. 2005. Glaciers and the changing earth system: a 2004 snapshot. Occasional paper 58, Institute of Arctic and Alpine Research, University of Colorado, Boulder, CO.

Eaton B, Moore R. 2010. Regional hydrology. In *Compendium of Forest Hydrology and Geomorphology in British Columbia, Land Management Handbook 66*, vol **1**, B.C., chap 4, Pike R, Redding T, Moore R, Winkler R, Bladon K (eds). Ministry of Forests and Range, Forest Science Program and FORREX Forum for Research and Extension in Natural Resources: Victoria, BC and Kamloops, BC, URL http://www.for.gov.bc.ca/hfd/pubs/docs/Lmh/Lmh66.htm

Elsner MM, Lan C, Voisin N, Deems JS, Hamlet AF, Vano JA, Mickelson KEB, Se-Yeun L, Lettenmaier DP. 2010. Implications of 21st century climate change for the hydrology of Washington State. *Climate Change* **102**(1/2): 225–260.

FAO. 1995. Digital soil map of the world. Dataset Version 3.5, Land and Water Development Division, Food and Agriculture Organization of the United Nations, Rome, Italy.

Farr TG, Rosen PA, Caro E, Crippen R, Duren R, Hensley S, Kobrick M, Paller M, Rodriguez E, Roth L, Seal D, Shaffer S, Shimada J, Umland J, Werner M, Oskin M, Burbank D, Alsdorf D. 2007. The shuttle radar topography mission. *Reviews of Geophysics* **45**(2): DOI: 10.1029/2005rg000183

Fernandes R, Butson C, Leblanc S, Latifovic R. 2003. Landsat-5 TM and landsat-7 ETM + based accuracy assessment of leaf area index products for Canada derived from SPOT-4 VEGETATION data. *Canadian Journal of Remote Sensing* **29**(2): 241–258.

Fleming SW, Whitfield PH. 2010. Spatiotemporal mapping of ENSO and PDO surface meteorological signals in British Columbia, Yukon, and southeast Alaska. *Atmosphere-Ocean* **48**(2): 122–131.

Fleming SW, Whitfield PH, Moore RD, Quilty EJ. 2007. Regime-dependent streamflow sensitivities to Pacific climate modes cross the Georgia-Puget transboundary ecoregion. *Hydrological Processes* **21**(24): 3264–3287.

Global Soil Data Task Group. 2000. Global gridded surfaces of selected soil characteristics (International Geosphere-Biosphere Programme – Data and Information System). Available on-line at http://www.daac.ornl.gov, DOI: 10.3334/ORNLDAAC/569

Gonzalez P, Neilson RP, Lenihan JM, Drapek RJ. 2010. Global patterns in the vulnerability of ecosystems to vegetation shifts due to climate change. *Global Ecology and Biogeography* **19**(6): 755–768.

Hamlet AF, Lettenmaier DP. 1999. Effects of climate change on hydrology and water resources in the Columbia River basin. *Journal of the American Water Resources Association* **35**(6): 1597–1623.

Hamlet AF, Lettenmaier DP. 2005. Production of temporally consistent gridded precipitation and temperature fields for the continental United States. *Journal of Hydrometeorology* **6**(3): 330–336.

Hamlet AF, Mote PW, Clark MP, Lettenmaier DP. 2005. Effects of temperature and precipitation variability on snowpack trends in the western United States. *Journal of Climate* **18**(21): 4545–4561.

Hamlet AF, Se-Yeun L, Mickelson KEB, Elsner MM. 2010. Effects of projected climate change on energy supply and demand in the Pacific Northwest and Washington State. *Climate Change* **102**(1/2): 103–128.

Hayhoe K, Cayan D, Field CB, Frumhoff PC, Maurer EP, Miller NL, Moser SC, Schneider SH, Cahill KN, Cleland EE, Dale L, Drapek R, Hanemann RM, Kalkstein LS, Lenihan J, Lunch CK, Neilson RP, Sheridan SC, Verville JH. 2004. Emissions pathways, climate change, and impacts on California. *Proceedings of the National Academy of Sciences of the United States of America* **101**(34): 12,422–12,427.

Helsel D, Hirsch R. 2002. Statistical methods in water resources. *Statistical Techniques of Water-Resources Investigations Book 4*, Chapter A3, U.S. Geological Survey. Available at http://pubs.usgs.gov/twri/twri4a3/ Accessed on December 11 2012.

Hock R, Jansson P, Braun LN. 2005. Modelling the response of mountain glacier discharge to climate warming. In *Global Change and Mountain Regions, Advances in Global Change Research*, vol **23**, Huber UM, Bugmann HKM, Reasoner MA (eds), Springer: Netherlands, pp 243–252.

Hollander M, Wolfe DA. 1999. *Nonparametric Statistical Methods*, 2nd edn. John Wiley and Sons: New York, NY.

Huang JG, Bergeron Y, Denneler B, Berninger F, Tardif J. 2007. Response of forest trees to increased atmospheric CO2. *Critical Reviews in Plant Sciences* **26**(5–6): 265–283.

Huss M, Jouvet G, Farinotti D, Bauder A. 2010. Future high-mountain hydrology: a new parameterization of glacier retreat. *Hydrology Earth System Sciences* **14**(5): 815–829, DOI: 10.5194/hess-14-815-2010

IPCC. 2007. Summary for policymakers. In *Climate Change 2007: The Physical Science Basis. Contribution of Working Group I to the Fourth Assessment Report of the Intergovernmental Panel on Climate Change*, Solomon S, Qin D, Manning M, Chen Z, Marquis M, Averyt K, Tignor M, Miller H (eds). Cambridge University Press, Cambridge: United Kingdom and New York, NY, USA, pp 1–18.

Jackson RB, Canadell J, Ehleringer JR, Mooney HA, Sala OE, Schulze ED. 1996. A global analysis of root distributions for terrestrial biomes. *Oecologia* **108**(3): 389–411.

JISAO. 2010. The Pacific Decadal Oscillation (PDO). URL http://jisao.washington.edu/pdo, last accessed 2 December 2010.

Jost G, Moore RD, Menounos B, Wheate R. 2011. Quantifying the contribution of glacier runoff to streamflow in the Upper Columbia River basin, Canada. *Hydrology Earth System Sciences Discussions* **8**: 4979–5008, DOI: 10.5194/hessd-8-4979-2011

K-1 Model Developers. 2004. K-1 coupled model (MIROC) description. K-1 Technical Report 1, Center for Climate System Research, University of Tokyo, Tokyo, Japan, URL http://www.ccsr.u-tokyo.ac.jp/kyosei/hasumi/MIROC/tech-repo.pdf

Kaser G, Cogley JG, Dyurgerov MB, Meier MF, Ohmura A. 2006. Mass balance of glaciers and ice caps: consensus estimates for 1961–2004. *Geophysical Research Letters* **33**(19): DOI: 10.1029/2006gl027511

Kienzle SW. 2008. A new temperature based method to separate rain and snow. *Hydrological Processes* **22**(26): 5067–5085.

Kim J. 2001. A nested modeling study of elevation-dependent climate change signals in California induced by increased atmospheric CO2. *Geophysical Research Letters* **28**(15): 2951–2954.

Knowles N, Cayan DR. 2004. Elevational dependence of projected hydrologic changes in the San Francisco estuary and watershed. *Climate Change* **62**(1–3): 319–336.

Knutti R, Abramowitz G, Collins M, Eyring V, Gleckler P, Hewitson B, Mearns L. 2010. Good practice guidance paper on assessing and combining multi model climate projections. In *Meeting Report of the Intergovernmental Panel on Climate Change Expert Meeting on Assessing and Combining Multi Model Climate Projections*, Stocker T, Qin D, Plattner GK, Tignor M, Midgley P (eds), IPCC Working Group I Technical Support Unit, University of Bern: Bern, Switzerland.

Leavesley GH. 1994. Modeling the effects of climate-change on water-resources – a review. *Climate Change* **28**(1–2): 159–177.

Liang X, Lettenmaier DP, Wood EF, Burges SJ. 1994. A simple hydrologically based model of land-surface water and energy fluxes for general-circulation models. *Journal of Geophysical Research-Atmospheres* **99**(D7): 14,415–14,428.

Liang X, Wood EF, Lettenmaier DP. 1996. Surface soil moisture parameterization of the VIC-2L model: evaluation and modification. *Global Planet Change* **13**(1–4): 195–206.

Lohmann D, NolteHolube R, Raschke E. 1996. A large-scale horizontal routing model to be coupled to land surface parametrization schemes. *Tellus Series A* **48**(5): 708–721.

Loukas A, Vasiliades L, Dalezios NR. 2002a. Climatic impacts on the runoff generation processes in British Columbia, Canada. *Hydrology Earth System Sciences* **6**(2): 211–227.

Loukas A, Vasiliades L, Dalezios NR. 2002b. Potential climate change impacts on flood producing mechanisms in southern British Columbia, Canada using the CGCMA1 simulation results. *Journal of Hydrology* **259**(1–4): 163.

Mantua N, Tohver I, Hamlet A. 2010. Climate change impacts on streamflow extremes and summertime stream temperature and their possible consequences for freshwater salmon habitat in Washington State. *Climate Change* **102**(1/2): 187–223.

Marlon JR, Bartlein PJ, Walsh MK, Harrison SP, Brown KJ, Edwards ME, Higuera PE, Powerh MJ, Anderson RS, Briles C, Brunelle A, Carcaillet C, Daniels M, Hu FS, Lavoie M, Long C, Minckley T, Richard PJH, Scott AC, Shafer DS. 2009. Wildfire responses to abrupt climate change in North America. *Proc Natl Acad Sci USA* **106**(8): 2519–2524.

Martin GM, Ringer MA, Pope VD, Jones A, Dearden C, Hinton TJ. 2006. The physical properties of the atmosphere in the New Hadley Centre Global Environmental Model (HadGEM1). Part I: model description and global climatology. *Journal of Climate* **19**: 1274–1301. DOI: 10.1175/JCLI3636.1.

Maurer EP, Hidalgo HG. 2008. Utility of daily vs. monthly large-scale climate data: an intercomparison of two statistical downscaling methods. *Hydrol Earth System Science* **12**(2): 551–563.

Maurer EP, Wood AW, Adam JC, Lettenmaier DP, Nijssen B. 2002. A long-term hydrologically based dataset of land surface fluxes and states for the conterminous United States. *Journal of Climate* **15**(22): 3237.

Meehl GA, Covey C, Delworth T, Latif M, McAvaney B, Mitchell JFB, Stouffer RJ, Taylor KE. 2007. The WCRP CMIP3 multimodel dataset: a new era in climate change research. *B Am Meteorol Soc* **88**(9): 1383–1394.

Merritt WS, Alila Y, Barton M, Taylor B, Cohen S, Neilsen D. 2006. Hydrologic response to scenarios of climate change in sub watersheds of the Okanagan basin, British Columbia. *Journal of Hydrology* **326**(1–4): 79–108.

Milly P, Betancourt J, Falkenmark M, Hirsch RM, Kundzewicz ZW, Lettenmaier DP, Stouffer RJ. 2008. Stationarity is dead: whither water management? *Science* **319**(5863): 573–574.

Moore RD, McKendry IG. 1996. Spring snowpack anomaly patterns and winter climatic variability, British Columbia, Canada. *Water Resources Research* **32**(3): 623–632.

Mote PW, Hamlet AF, Clark MP, Lettenmaier DP. 2005.erican Declining mountain snowpack in western North America. *Bulletin of the Am Meteoroligical Society* **86**(1): 39–49.

Mote PW, Parson E, Hamlet AF, Keeton WS, Lettenmaier D, Mantua N, Miles EL, Peterson D, Peterson DL, Slaughter R, Snover AK. 2003. Preparing for climatic change: the water, salmon, and forests of the Pacific Northwest. *Clim Change* **61**(1–2): 45–88.

Nakićenović N, Swart R (eds). 2000. Emissions scenarios. *IPCC Special Reports*, Cambridge University Press: Cambridge, UK.

Nijssen B, O'Donnell GM, Hamlet AF, Lettermaier DP. 2001. Hydrologic sensitivity of global rivers to climate change. *Climate Change* **50**(1/2): 143–175.

Payne JT, Wood AW, Hamlet AF, Palmer RN, Lettenmaier DP. 2004. Mitigating the effects of climate change on the water resources of the Columbia River basin. *Climate Change* **62**(1–3): 233–256.

Pierce DW, Barnett TP, Hidalgo HG, Das T, Bonfils C, Santer BD, Bala G, Dettinger MD, Cayan DR, Mirin A, Wood AW, Nozawa T. 2008. Attribution of declining western U.S. snowpack to human effects. *Journal of Climate* **21**(23): 6425–6444.

Pietroniro A, Leconte R, Toth B, Peters DL, Kouwen N, Conly FM, Prowse T. 2006. Modelling climate change impacts in the Peace and Athabasca catchment and delta: III – integrated model assessment. *Hydrological Processes* **20**(19): 4231–4245.

Prudhomme C, Davies H. 2009. Assessing uncertainties in climate change impact analyses on the river flow regimes in the UK. Part 2: future climate. *Climate Change* **93**(1/2): 197–222.

Quick M. 1995. The UBC watershed model. In *Computer Models in Watershed Hydrology*, chap 8, Singh V (ed). Water Resources Publications: Highlands Ranch, CO.

Regonda SK, Rajagopalan B, Clark M, Pitlick J. 2005. Seasonal cycle shifts in hydroclimatology over the western United States. *Journal of Climate* **18**(2): 372–384.

Roberts J. 2000. The influence of physical and physiological characteristics of vegetation on their hydrological response. *Hydrological Processes* **14**(16–17): 2885–2901.

Roeckner E, Brokopf R, Esch M, Giorgetta M, Hagemann S, Kornblueh L, Manzini E, Schlese U, Schulzweida U. 2006. Sensitivity of simulated climate to horizontal and vertical resolution in the ECHAM5 atmosphere model. *Journal of Climate* **19**(16): 3771–3791. DOI: 10.1175/JCLI3824.1

Romolo L, Prowse TD, Blair D, Bonsal BR, Martz LW. 2006. The synoptic climate controls on hydrology in the upper reaches of the Peace River basin. Part I: snow accumulation. *Hydrological Processes* **20**(19): 4097–4111.

Rotstayn LD, Collier MA, Dix MR, Feng Y, Gordon HB, O'Farrell SP, Smith IN, Syktus J. 2010. Improved simulation of Australian climate and ENSO-related rainfall variability in a global climate model with an interactive aerosol treatment. *International Journal of Climatology* **30**(7): 1067–1088. DOI: 10.1002/joc.1952

Salathé EP. 2005. Downscaling simulations of future global climate with application to hydrologic modelling. *International Journal of Climatology* **25**(4): 419–436.

Schiefer E, Menounos B, Wheate R. 2007. Recent volume loss of British Columbian glaciers, Canada. *Geophysical Research Letters* **34**(16): DOI: 10.1029/2007gl030780

Schindler DW, Donahue WF. 2006. An impending water crisis in Canada's western prairie provinces. *Proceedings of the National Academy of Sciences of the United States of America* **103**(19): 7210–7216.

Schnorbus MA, Bennett KE, Arelia WT, Berland AJ. 2011. Hydrologic impacts of climate change in the Peace, Campbell and Columbia Watersheds, British Columbia, Canada. Pacific Climate Impacts Consortium, University of Victoria, Victoria, BC, URL http://pacificclimate.org/sites/default/files/publications/Schnorbus.HydroModelling.FinalReport2.Apr2011.pdf

Schnorbus M, Bennett K, Werner A. 2010. Quantifying the water resource impacts of mountain pine beetle and associated salvage harvest operations across a range of watershed scales: hydrologic modelling of the Fraser River basin. Information Report BC-X-423, Natural Resources Canada, Canadian Forest Service, Pacific Forestry Centre, Victoria, BC.

Scinocca JF, McFarlane NA, Lazare M, Li J, Plummer D. 2008. Technical note: the CCCma third generation AGCM and its extension into the middle atmosphere. *Atmospheric Chemistry and Physics* **8**(23): 7055–7074, DOI: 10.5194/acp-8-7055-2008.

Shuttleworth WJ. 1993. Evaporation. In *Handbook of Hydrology*, chap 4, Maidment DR (ed). McGraw-Hill: New York, NY.

Smithson P, Addison K, Atkinson K. 2002. *Fundamentals of the Physical Environment*, 3rd edn. Routledge: London, UK and New York, NY.

Stahl K, Moore RD. 2006. Influence of watershed glacier coverage on summer streamflow in British Columbia, Canada. *Water Resources Research* **42**(6): DOI: 10.1029/2006wr005022

Stahl K, Moore RD, Floyer JA, Asplin MG, McKendry IG. 2006. Comparison of approaches for spatial interpolation of daily air temperature in a large region with complex topography and highly variable station density. *Agricultural and Forest Meteorology* **139**(3/4): 224–236.

Stahl K, Moore RD, Shea JM, Hutchinson D, Cannon AJ. 2008. Coupled modelling of glacier and streamflow response to future climate scenarios. *Water Resources Research* **44**(2): W02422, DOI: 10.1029/2007WR005966

Toth B, Pietroniro A, Conly FM, Kouwen N. 2006. Modelling climate change impacts in the Peace and Athabasca catchment and delta: I – hydrological model application. *Hydrological Processes* **20**(19): 4197–4214.

Vano JA, Scott MJ, Voisin N, Stöckle CO, Hamlet AF, Mickelson KEB, Elsner MM, Lettenmaier DP. 2010a. Climate change impacts on water management and irrigated agriculture in the Yakima River Basin, Washington, USA. *Climate Change* **102**(1/2): 287–317.

Vano JA, Voisin N, Cuo L, Hamlet AF, Elsner MM, Palmer RN, Polebitski A, Lettenmaier DP. 2010b. Climate change impacts on water management in the Puget Sound region, Washington State, USA. *Climate Change* **102**(1–2): 261–286.

VanRheenen NT, Wood AW, Palmer RN, Lettenmaier DP. 2004. Potential implications of PCM climate change scenarios for Sacramento-San Joaquin River Basin hydrology and water resources. *Climate Change* **62**(1–3): 257–281.

Wang T, Hamann A, Spittlehouse DL, Aitken SN. 2006. Development of scale-free climate data for western Canada for use in resource management. *International Journal of Climatology* **26**(3): 383–397.

Werner AT. 2011. BCSD downscaled transient climate projections for eight select GCMs over British Columbia, Canada. Pacific Climate Impacts Consortium, University of Victoria, Victoria, BC, URL http://pacificclimate.org/sites/default/files/publications/Werner.HydroModelling.FinalReport1.Apr2011.pdf

Whitfield PH, Cannon AJ. 2000. Recent variations in climate and hydrology in Canada. *Canadian Water Resources Journal* **25**(1): 19–65.

Whitfield PH, Cannon AJ, Reynolds CJ. 2002. Modelling streamflow in present and future climates: examples from the Georgia Basin, British Columbia. *Canadian Water Resources Journal* **27**(4): 427–456.

Wilby RL. 2005. Uncertainty in water resource model parameters used for climate change impact assessment. *Hydrological Processes* **19**(16): 3201–3219.

Wood AW, Leung LR, Sridhar V, Lettenmaier DP. 2004. Hydrologic implications of dynamical and statistical approaches to downscaling climate model outputs. *Climate Change* **62**(1–3): 189–216.

Wood AW, Maurer EP, Kumar A, Lettenmaier DP. 2002. Long-range experimental hydrologic forecasting for the eastern United States. *Journal of Geophysical Research-Atmospheres* **107**(D20): DOI: 10.1029/2001jd000659

Wulder MA, Dechka JA, Gillis MA, Luther JE, Hall RJ, Beaudoin A. 2003. Operational mapping of the land cover of the forested area of Canada with Landsat data: EOSD land cover program. *The Forestry Chronicle* **79**(6): 1075–1083.

Yapo PO, Gupta HV, Sorooshian S. 1998. Multi-objective global optimization for hydrologic models. *Journal of Hydrology* **204**(1–4): 83–97.

